This document was prepared for the ETI by third parties under contract to the ETI. The ETI is making these documents and data available to the public to inform the debate on low carbon energy innovation and deployment.

Programme Area: Marine

Project: PerAWAT

Title: Calibration Report for Scale Model Experiments

Abstract:

This report details calibration of the experimental flow conditions, rotor and electro-mechanical systems for the equipment described in WG4 WP2 D2. Measurements are presented of the flow structure, of the characteristic of the small-scale rotor and of the structure of the wake of a single turbine and pair of turbines. The information presented demonstrates that the planned turbine tests can be calibrated correctly.

Context:

The Performance Assessment of Wave and Tidal Array Systems (PerAWaT) project, launched in October 2009 with £8m of ETI investment. The project delivered validated, commercial software tools capable of significantly reducing the levels of uncertainty associated with predicting the energy yield of major wave and tidal stream energy arrays. It also produced information that will help reduce commercial risk of future large scale wave and tidal array developments.

PerAWAT WG4 WP2 D4(b)
Calibration report for Scale Model Experiments

Project	PerAWAT
Work package	WG4
Deliverable	WG4 WP2 D4 (b) Calibration report for Scale Model Experiments
Responsible author	Tim Stallard, Ralph Collings,
Second reading	Mat Thomson, Tong Feng
Circulation	UoM / GH
To be approved by	Robert Rawlinson-Smith (GH)
Date	01 February 2011
Issue	Version 1

Document revision history

Issue	Date	Summary
V1.0	01/02/2011	Version sent to ETI

EXECUTIVE SUMMARY

The first deliverable in this work package, WG4 WP2 D1, explains the data required from experimental study of an array of tidal stream devices. The second deliverable, WG4 WP2 D2, details the design of equipment required to conduct the experiments. Topics covered include the generation of ambient flow conditions, method of measurement of time-varying flow- and mechanical parameters, design of small-scale model of a tidal stream turbine and design of a rotor suitable for the low Reynolds number of these experiments ($3x10^4$ approx.). Engineering drawings are supplied for the main items of equipment. The third deliverable provides a summary of the equipment that has been installed and purchased. Photographs were provided of the main items of equipment detailed in WG4 WP2 D2. A modified dynamometer design was also described which comprises a bevel gear and motor mounted vertically above waterline. This report constitutes WG4WP2 D4 and details calibration of the experimental flow conditions, rotor and electro-mechanical systems. Measurements are presented of the flow structure, of the characteristic of the small-scale rotor and of the structure of the wake of a single turbine and pair of turbines. The information presented demonstrates that the planned turbine tests can be calibrated correctly.

CONTENTS

1 INTRODUCTION

1.1 Scope of this document

This document constitutes the third deliverable (D4) of working group 4, work package 2 (WG4WP2) of the PerAWAT (Performance Assessment of Wave and Tidal Arrays) project funded by the Energy Technologies Institute (ETI). The project partners of this work package are the University of Manchester (UoM) and Garrad Hassan (GH). This work package addresses the influence of bounding surfaces (seabed, other devices and free surface) and on the characteristics of the incident flow on performance, loading and wake structure. These issues are addressed by a series of small-scale experiments in which an array of tidal stream turbine rotors are studied in a wide channel. The tests are conducted at approximately 1:70th geometric scale using rotors that are specifically designed to produce similar momentum extraction to a generic full-scale rotor design. Earlier deliverables explain the scaling considerations that influence the design of the tests, the specification of the experimental equipment and both the design and construction of experimental equipment.

In this report, the calibration process is detailed both for individual items of equipment and for normalisation of measured data. Summary information is presented regarding the structure of the ambient flow for the standard case of an average flow velocity of 0.45 m/s and for modifications due to waves and, separately, the oscillating flow downstream of an immersed island. The calibration method is explained for the dynamometer used for the array tests. The calibrated equipment is employed to measure the loading and wake structure associated with a single rotor demonstrating that the processes employed allow calibration of the array tests.

1.2 Specific tasks associated with WG4 WP2

- Test specification of sufficient detail and scope (D1) to: Evaluate the effect of bounding surfaces and device performance characteristics on the device loading. Evaluate the effect of bounding surfaces, ambient flow field and device performance characteristics on the far wake form. Investigate the wake interactions within an array including influence of varying ambient turbulence intensities (seabed, waves and large eddies). Specification will define the details of: operating points (speeds/torques), instrument type, sample frequencies, acceptable error and experimental programme plan.

- Design of test equipment (D2) [GH & UoM]: This document provides a description of the design methodology for the main items of experimental equipment. Details are given of the approach used for generating the range of flow conditions required, and for measurement of flow characteristics at the temporal and spatial resolution required. The dimensions and component specification of the turbine model are summarised and the rotor design process detailed. An overview is also given of the calibration, data collection and data logging procedures that will be implemented.

- Construction of test equipment (D3) [UoM] including: Rotor (blades, hub, nacelle, generator), Instrumentation system, Support structure, and Alteration to facility equipment.

- Calibration of test equipment for physical scale tests (D4) [UoM&GH] including: flow profile, depth, ambient turbulence and waves. A database of calibration data and summary report will be produced summarising the key calibration tests and results such that turbine tests can be correctly calibrated.

- Conduct physical scale model tidal tank tests, issue database of experimental data and testing report (D5) [GH], including; Data post processing for presentation in experimental database

(filtering, quality control etc.), Issue database of experimental data obtained under different current, wave and turbulence conditions

1.3 Experimental Programme

The objectives of WG4WP2, as set out in Schedule 5, are to investigate (through physical testing of an array of up to 15 small devices):

1. the effect of bounding surfaces (free surface, seabed and other devices) on device performance and loading
2. the effect of the bounding surfaces, ambient flow field and device performance characteristics on the far wake form
3. the wake interactions within an array including influence of varying ambient turbulence intensities (seabed, waves and large eddies)

These investigations will be conducted by measuring the rotor loading and wake structure for several array configurations. An outline of the test programme was given in WG4WP2D2. For each array configuration, velocity measurements will be obtained along the axial centreline and a horizontal and vertical traverse of the wake will be conducted at several downstream distances. The location of the measurement co-ordinates for the principal array configurations is shown in Figure. A list of the experiments and range of measurement positions is given in Appendix B.

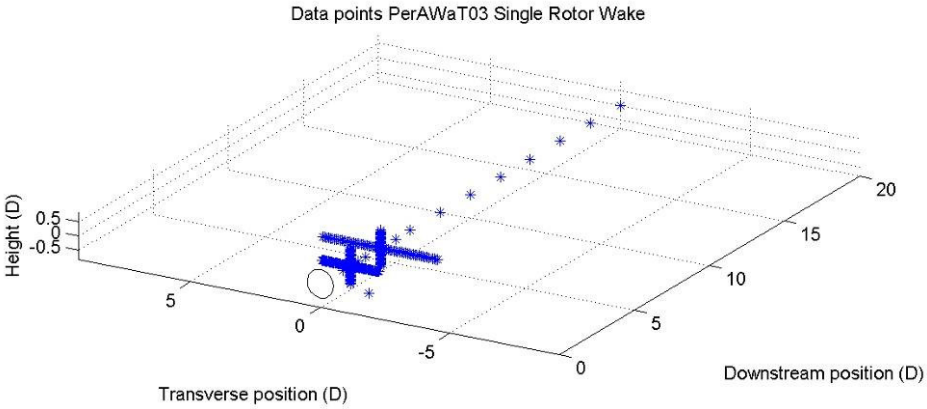

(a) Single wake measurement (see also Section 5)

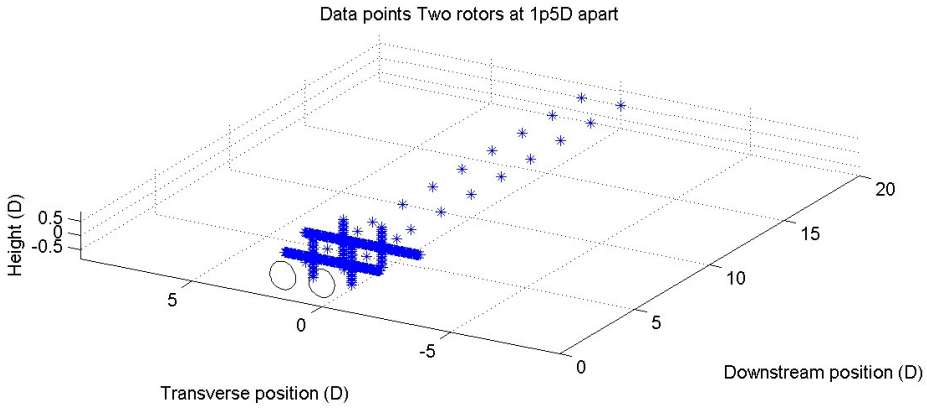

(b) Two rotor blockage study. – lateral spacings of 1.5D, 2D and 3D (see also Section 5.3).

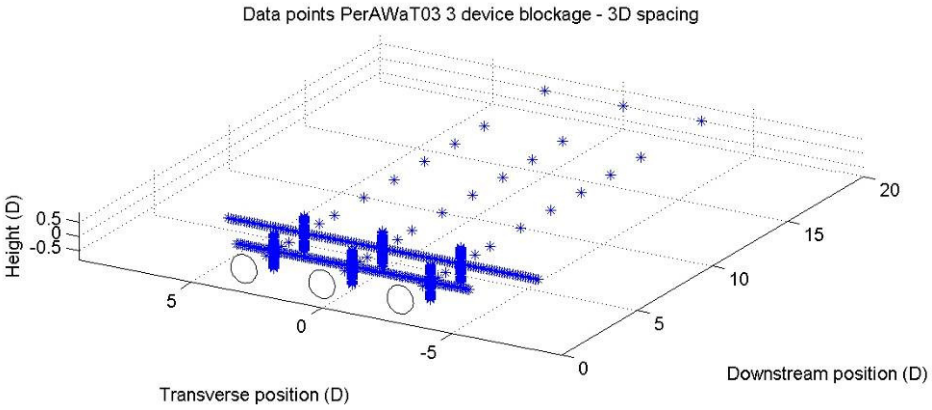

(c) Three rotor blockage study. – lateral spacings of 1.5D, 2D and 3D.

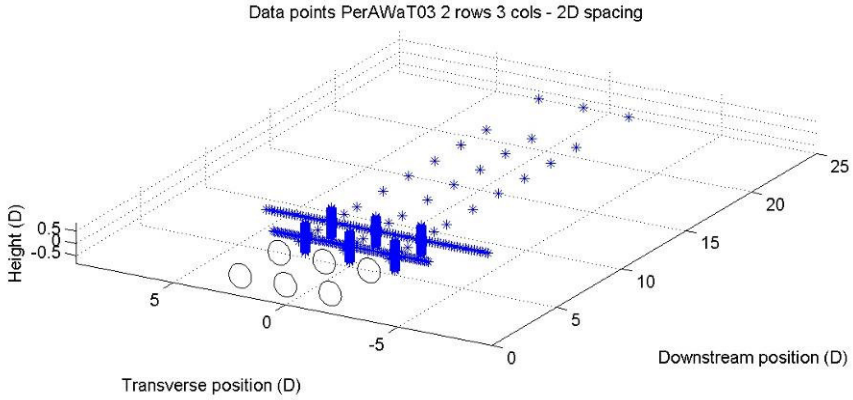

(d) Two row study – rotors at lateral spacing of 2 D and row spacing of 3 D, 4D, 5D and 6D. Effect of waves, oscillating flow and increased turbulence due to bed roughness also studied.

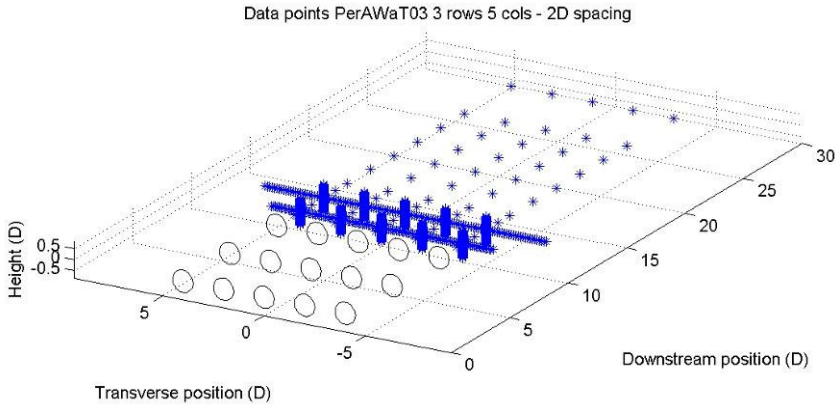

(e) Three row study – rotors at lateral spacing of 2D.

Figure 1.1: Indicative arrangement of measurement positions downstream of the principal array configurations. Velocities are measured downstream of the final row of the array. Longitudinal traverse is conducted over the range 0D < X < 10D relative to the rotor plane. Vertical traverses aligned with rotor centreline and horizontal traverse at hub height across width of wake.

2 DEFINITIONS

A flow field is defined by three components of velocity aligned with the global co-ordinate system (U, V, W) = (U_x, U_y, U_z) where the X-axis is aligned to the direction of flow, Y the lateral component and Z the vertical component. At each x, y, z ordinate time varying velocity is measured as e.g.:

$$U(x,y,z,t)$$

Time averaged velocity is defined as

$$U(x,y,z,t) = \overline{U(x,y,z)}$$

Velocity is normalised to either the baseflow at hub height ($U_{0,h}$) or to the baseflow at the same co-ordinate; either at the same depth ($U_0(z)$) or the same lateral position (U0(y)), e.g:

$$U_{n0h} = \frac{U(x,y,z)}{U_{0,h}}$$

$$U_{n0}(z) = \frac{U(x,y,z)}{U_0(z)} \text{ or } U_{n0}(y) = \frac{U(x,y,z)}{U_0(y)}$$

Velocity deficit is also defined relative either to the baseflow at hub heigh

normalised baseflow (inflow) hub height Uoh

$$U_{d0h} = \frac{U(x,y,z) - U_{0,h}}{U_{0,h}}$$

normalised base flow depth profile Uo(z)

$$U_{d0}(z) = \frac{U(x,y,z) - U_0(z)}{U_0(z)}$$

For this study the lateral profile of the baseflow is assumed to be uniform (see Section 3) in Y and so Unoh, Unoz, Udoh and Udoz are of particular interest.

Several turbulence parameters are of interest including the turbulence intensity and several components of the Reynolds stress. Time-varying turbulent fluctuations are defined as:

$$u = U - \overline{U}$$

where u, v, w are the turbulent fluctuations of velocity in the x,y,z direction and the overbar indicates the time averaged value. Turbulent kinetic energy (TKE) per unit volume of fluid is

$$TKE = \rho\frac{\overline{u^2} + \overline{v^2} + \overline{w^2}}{2} = \rho\frac{\overline{q^2}}{2}$$

Relative turbulence intensity (u'), also referred to as third moment of turbulence, is defined as the standard deviation of the turbulence fluctuation normalised to a component of velocity:

$$u' = \frac{\sqrt{\overline{u^2}}}{\overline{U}}$$

Similarly, turbulence intensity (TI) is defined as the standard deviation of the turbulence fluctuation normalised to the flow speed (Q). For the x-direction this is written:

$$TIx = \frac{\sqrt{\overline{u^2}}}{Q} * 100$$

Equivalent expressions are written in v for TIy and w for TIz where time averaged speed is:

$$Q = \sqrt{\overline{U}^2 + \overline{V}^2 + \overline{W}^2}$$

The Reynolds stress occurs from the cross correlation of orthogonal velocity components. The lateral $\overline{\tau}_{yx}$ and vertical $\overline{\tau}_{zx}$ Reynolds Stresses are of particular interest:

$$\overline{\tau}_{yx} = \mu\frac{\partial\overline{V}}{\partial x} - \rho\overline{vu} \qquad \overline{\tau}_{zx} = \mu\frac{\partial\overline{W}}{\partial x} - \rho\overline{wu}$$

Since the molecular viscosity term will be small (of order of e.g. $\mu = 10^{-4}$ and max(dU/dy) < 1) relative to the cross correlation term (of order of 0.01 hence several orders of magnitude larger), only the cross correlation is considered in this study:

$$\overline{\tau}_{yx} \sim -\rho\overline{vu} \qquad \overline{\tau}_{zx} \sim -\rho\overline{wu}$$

3 AMBIENT FLOW CONDITIONS

This section provides details on the spatial variation of the velocity field in the University of Manchester wide flume prior to deployment of scale model tidal-stream devices. The general arrangement of the flume is briefly described in Section 3.1 and sample duration and quality discussed in Section 3.2. In Sections 3.3 – 3.5, the spatial variation of mean velocity and turbulence intensity is reported for three flow conditions: i) uniform flow, ii) uniform flow with waves and iii) flow past a conical island. Turbulence spectra are reported at co-ordinates corresponding to a rotor centre and to a point in the rotor wake.

3.1 General description of experimental equipment

The range of experimental studies required are summarised in Section 4.4 of WG4WP2D1. Most tests will be conducted at a comparable mean incident flow velocity but different depth profiles and turbulence characteristics will be studied. The tests were conducted in the University of Manchester wide flume at a water depth of 0.45 m. The flume is 5 m wide and the test section is 12 m in length. A porous weir has been installed at the inflow as detailed in WG4WP2D3. For all tests the fixed pitch rotor of diameter D = 270 mm is located at mid-depth and the first row located at X = 6 m measured from the inflow weir (Figure 3.1 and Figure 3.2). A left-handed global co-ordinate system is used in which X is aligned with the direction of the flow, Y is horizontal across the width of the flume and z is vertical (positive upwards). Data is presented either:

- in terms of absolute position relative to the origin of the flume: (X, Y, Z) = (0, 0, 0) located at the bottom left of the inflow weir in the positive X direction or,
- in terms of non-dimensional position relative to the centre of a rotor (i.e. in multiples of rotor diameter D = 270 mm) or to the flow depth (i.e. in multiples of flow depth h = 450 mm).

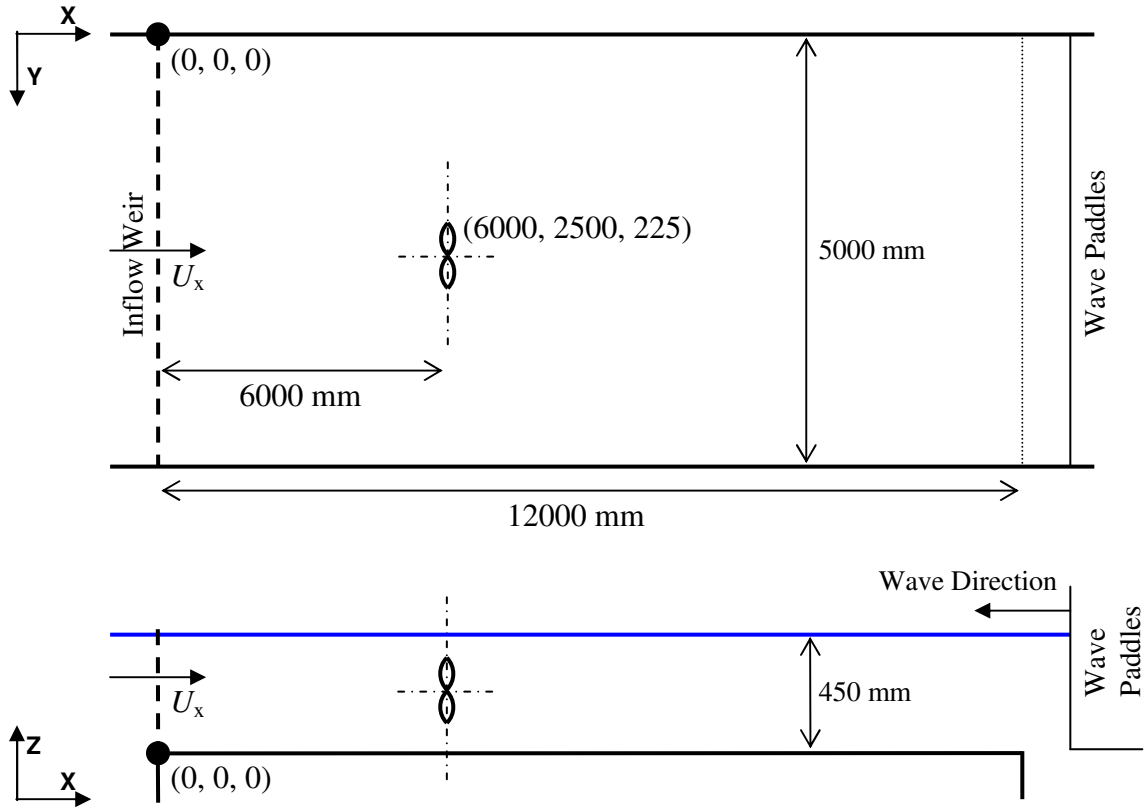

Figure 3.1: Longitudinal arrangement of flume indicating key dimensions and global co-ordinate system. NOT TO SCALE.

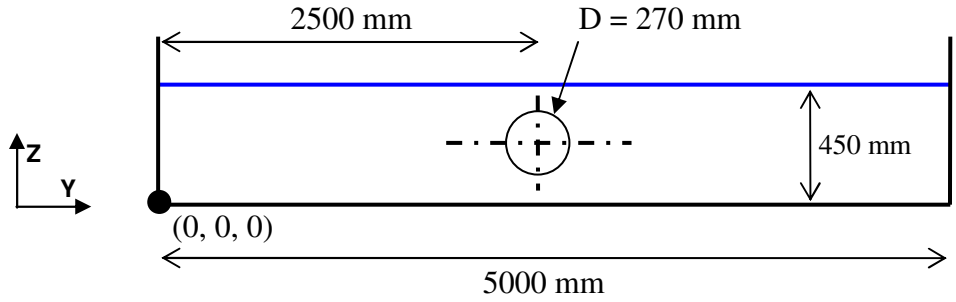

Figure 3.2: Lateral arrangement of flume indicating key dimensions and global co-ordinate system. NOT TO SCALE.

3.2 Analysis of Velocity Measurements

The majority of flow measurements comprise 12000 samples recorded at 200 Hz. A 60 second sample period is sufficient for mean values of velocity and turbulence intensity to be calculated to within ±2% approx. and for cross correlation to be converged to within ±5% approx (see Figure 3.3). As described in WG4WP2D2 and D3, the time-history of velocities and mechanical parameters are recorded using a Labview interface rather than the PolySync software provided with the ADVs. Magnitudes of signal to noise ratio (SNR) and correlation coefficient (COR) are therefore not recorded for each sample. However, these parameters are dependent on flow seeding and probe arrangement and so are not expected to vary during a test. Signal quality is measured prior to each test and typically indicate that the majority of samples (>95%) have SNR > 15 dB and COR > 50% (see Figure 3.4).

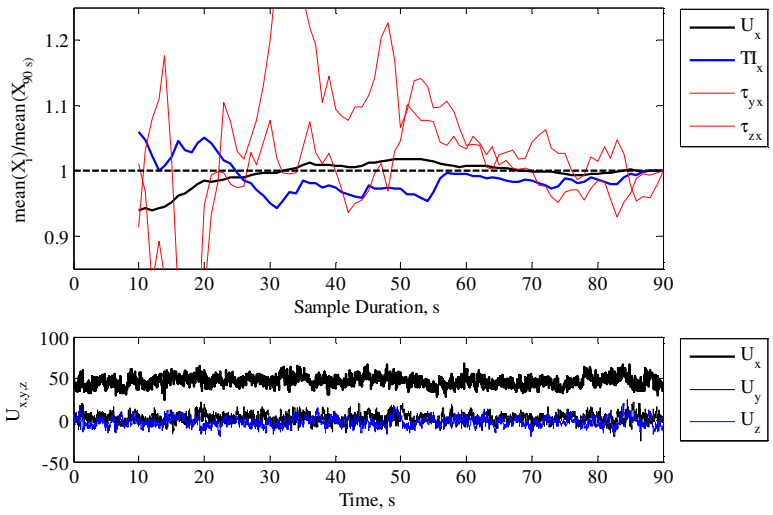

Figure 3.3: Convergence of mean values (of Ux, TIx and Lateral and vertical Reynolds stresses) with sample duration for a continuous 90 s sample at 200 Hz.

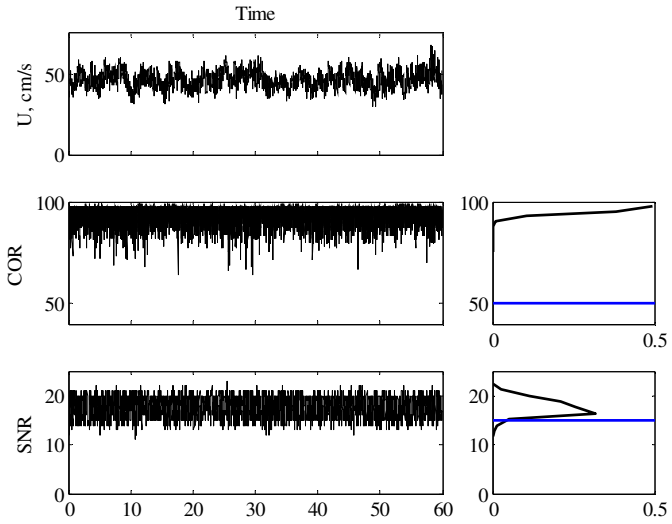

Figure 3.4: Typical time history of axial velocity (Ux) and corresponding signal to noise ratio (SNR) and correlation coefficient (COR). Data recorded using NORTEK Polysync sampling at 200 Hz. Histograms of COR and SNR also shown with threshold of COR > 50% and SNR > 15 dB indicated.

3.3 Steady Flow Generated Using Inflow Weir Only

Target flow conditions are identified in WG4 WP2 D1 Section 2.1 as:

Mean flow velocity ~ 0.45 m/s
Turbulence intensity ~ 10%

For all rotor tests the first line of devices is located at X = 6 m with subsequent lines of devices located at up to 10 D longitudinal spacing. Flow velocities have been measured at three longitudinal sections of the flume to quantify the incident flow and the flow across the extent of the array and wake. The sections considered are X = 6 m, 7.5 m and 9 m representing the first row of devices, approximately 5D downstream of the first row of devices and approximately 10D downstream of the first row of rotors. Between three and five devices will be deployed on each row of an array (see WG4WP2D2) and so the overall width of the array (outer tip to outer tip) will be approximately 2.1 m. The ADV measurement positions for each cross section of the flow comprise nine depth profiles of 18 z-ordinates and lateral profiles of 18 y-ordinates. The measurement co-ordinates for the baseflow are shown in Figure 3.5.

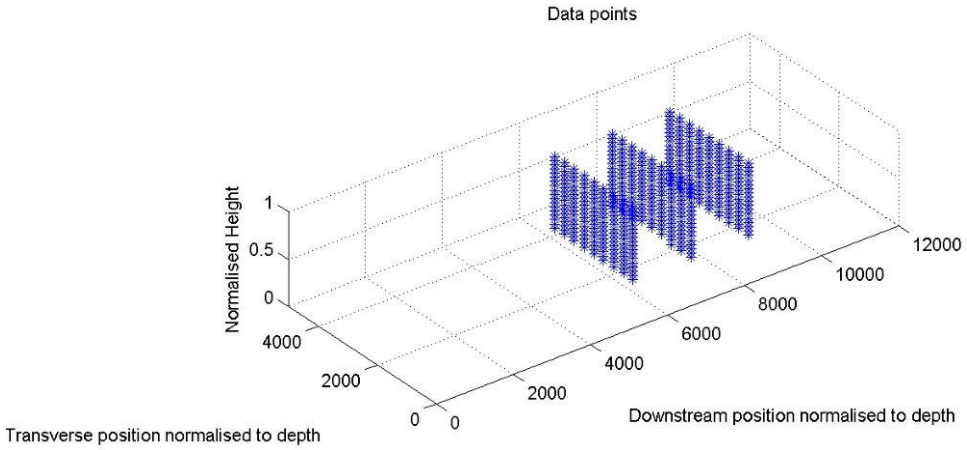

Figure 3.5: Baseflow measurement co-ordinates comprising 18 depth profiles on each of three sections

A summary of the longitudinal, transverse and depth-variation of flow is given by Figure 3.6 -Figure 3.11. Figures showing the spatial variation of other components of velocity (Uy, Uz) and turbulence intensity (TIy, TIz), in addition to Skewness, Kurtosis and Turbulent kinetic energy (see Appendix A) have also been produced and are located in the online database.

The flow velocity at each of the cross sections studied is approximately 45 cm/s with turbulence intensity of approximately 10% (Figure 3.6). Array tests require installation of rotors within the central 2 m width of the flume and over this region there is typically less than 3 cm/s variation of longitudinal velocity and less than 2% variation of turbulence intensity. Outside this region slightly greater variation of velocity and turbulence intensity is observed with marginally lower flow velocity and turbulence intensity at the left hand side of the flow (UY < 1500 mm) than the right hand side (Y > 3500 mm. Approximately 600 mm either side of the centreline (Y=2500 mm) of the flume, small regions of lower flow velocity are observed and correspond to regions of transverse circulation within the flow (Figure 3.7). The transverse flow velocities (Uy and Uz) in these regions is less than 3 cm/s so are not expected to influence rotor loading or wake recovery.

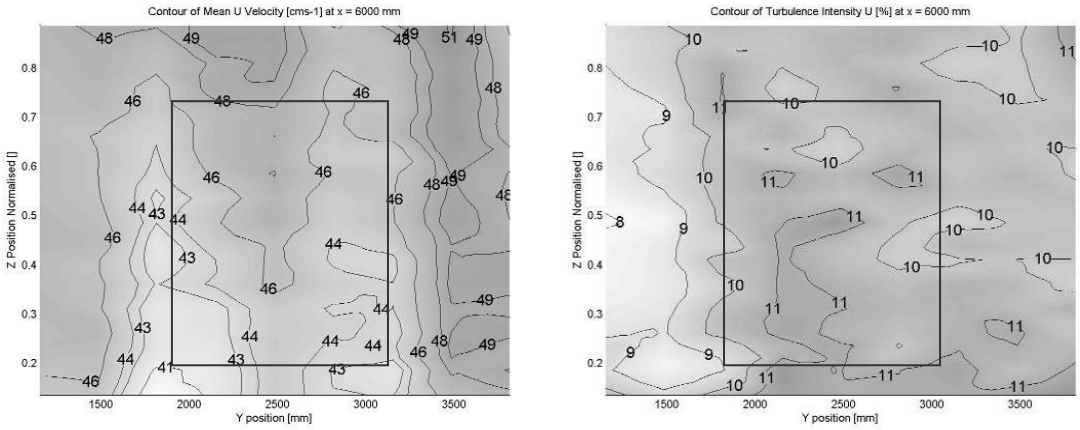

(a) X = 6.0 m.

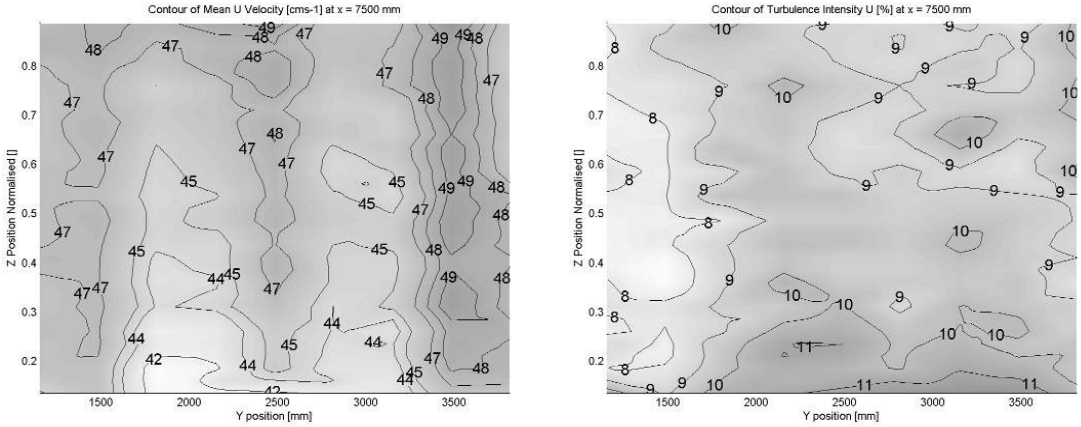

(b) X = 7.5 m

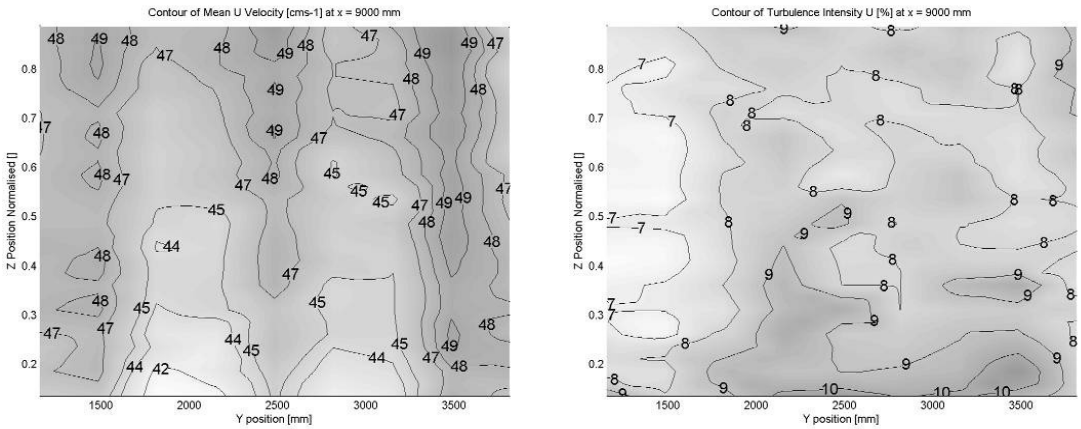

(c) X = 9.0 m

Figure 3.6: Contour plot of (Left) axial velocity (U, cm/s) and (Right) turbulence intensity TIx at X = 6 m from inlet (corresponding to first line of rotors), X = 7.5 m and X = 9.0 m

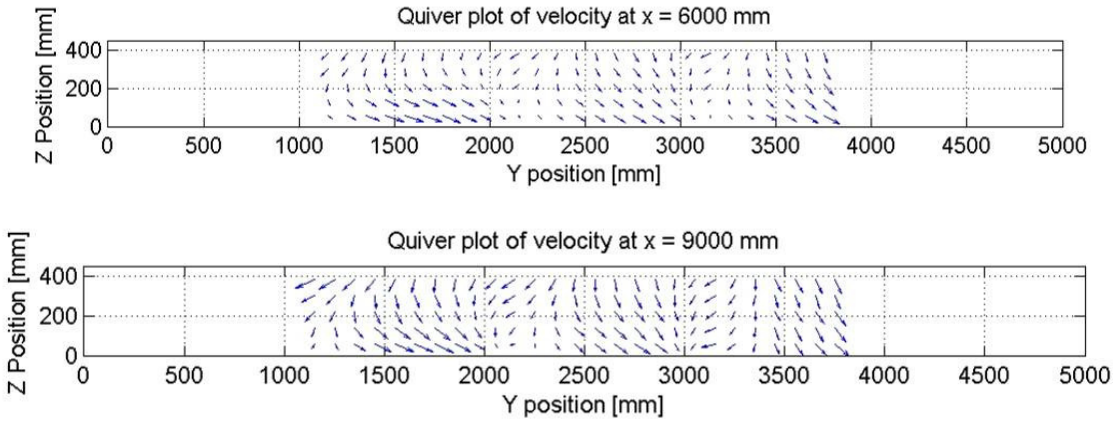

Figure 3.7: Velocity vectors (Uy, Uz) across section of flume at X = 6 m, and 9 m. Vectors shown correspond to 45 of the data points shown in Figure 3.5 and to co-ordinates interpolated between a total of 162 measurement points. Maximum Uy ~ 4 cm/s and maximum Uz ~ 3 cm/s (< 10% of mean longitudinal velocity ~ 45 cm/s).

The contour plots of Figure 3.6 indicate that the spanwise variation of velocity is relatively small, particularly across the extent of the array and so can be neglected. Depth profiles are similar at all three sections of the flow (Figure 3.8). For the purpose of normalising flow measurements, an average depth profile has been obtained as the mean velocity measured at each depth (Figure 3.9). A polynomial best-fit to the data has been obtained to normalise measurements at arbitrary depth. This is employed in Section 5.2 to analyse the structure of the wake of a single rotor.

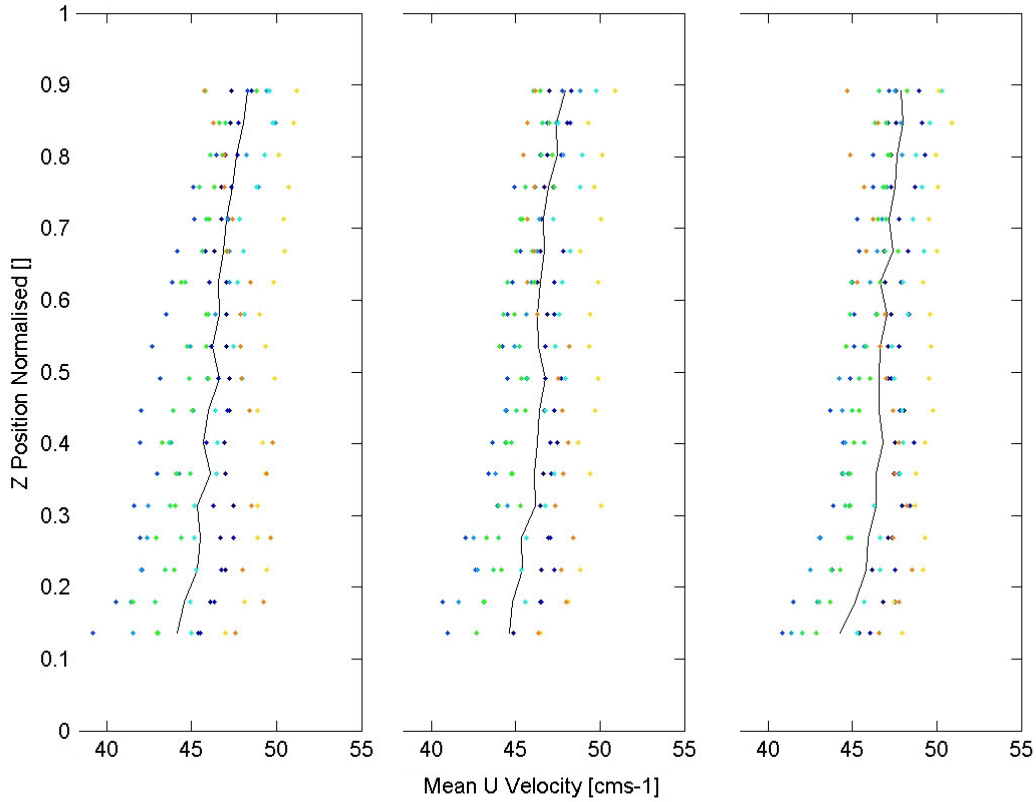

Figure 3.8: Depth-profile of axial velocity $U_x(z)$ at X = 6 m, 7.5 m and 9.0 m (from left to right respectively).

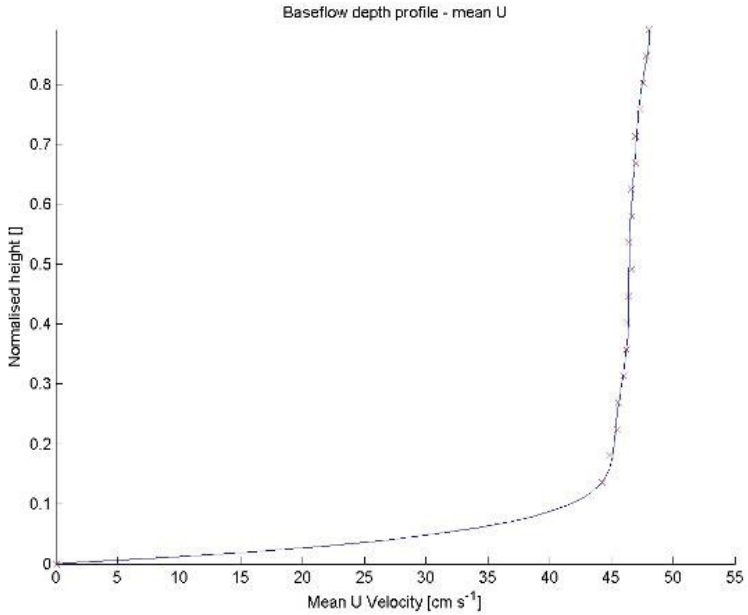

Figure 3.9: Averaged depth profile obtained as mean of all measurements at each depth at X = 6 m and used as baseflow for normalising wake measurements (see Section 5).

Turbulence intensity is close to constant across the water depth at X = 6 m but appears to dissipate with distance along the flume. Between X = 6 m and X = 9 m turbulence intensity reduces from an average of 10% to 8% (Figure 3.10). This is also reflected in a reduction of turbulent kinetic energy between X = 6 m and X = 9 m (Figure 3.11). This indicates that the turbulence developed by the inflow weir continues to dissipate over the length of the flume. However, such small variation is considered acceptable for these tests.

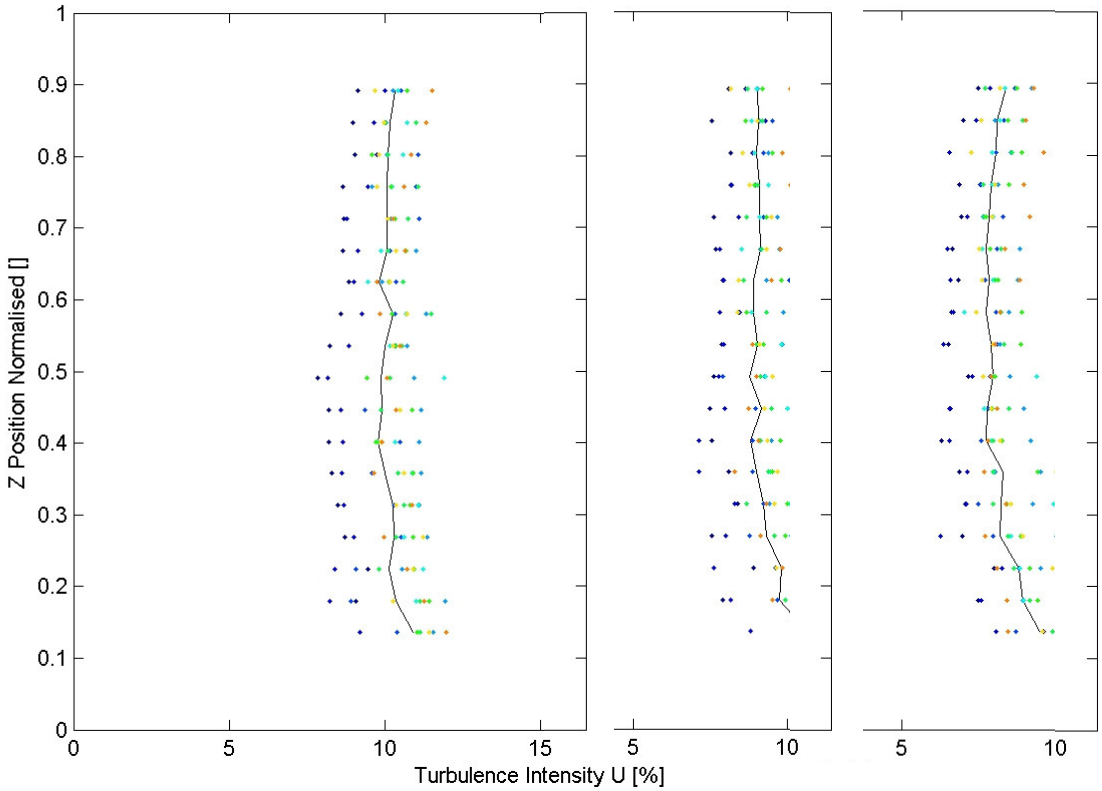

Figure 3.10: Depth-profile of turbulence intensity at X = 6 m, 7.5 m and 9.0 m (from left to right respectively).

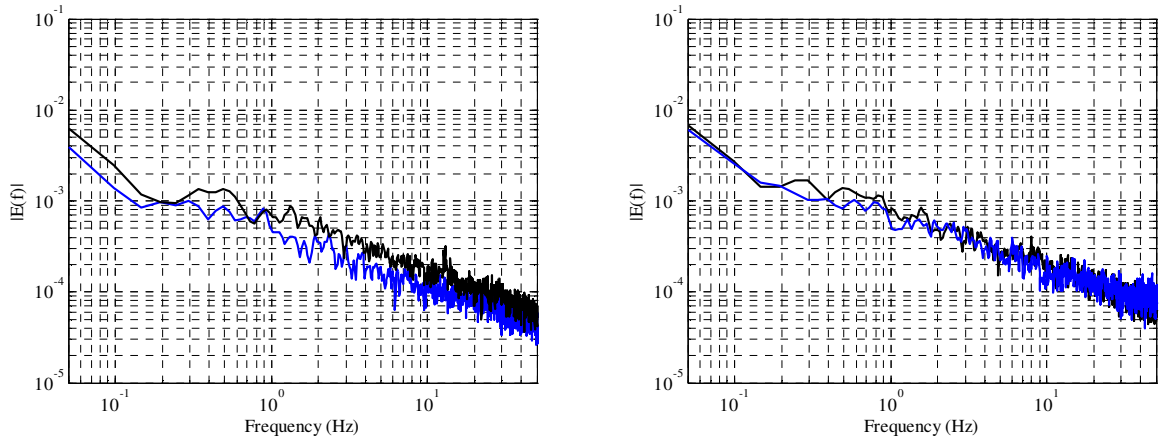

(a) Mid-depth at X = 6 m (black) and X = 9 m (blue)

(b) Near-bed (black) and near-surface (blue) at X = 6 m.

Figure 3.11: Longitudinal and depth variation of spectrum of Turbulent Kinetic Energy.

3.4 Steady Flow and Opposing Waves

Free-surface waves represent a source of flow turbulence that may significantly impact on the wake recovery process. For several array configurations, the effect of waves on the wake structure is therefore considered. Waves are generated using a position controlled wave paddle by Edinburgh Designs. Surface elevation is measured using capacitance type wave gauges. Each gauge is calibrated prior to the test by measurement of output voltage corresponding to several increments of immersion in still water. This provides a linear constant specific to each wave gauge.

WG4WP2D2 indicates that conditions representative of a tidal stream site would be considered subject to investigation of the range of achievable wave states in the University of Manchester flume. Assuming a Bretschneider spectrum (for which $T_z \sim 0.78T_p$) zero-crossing periods at the EMEC site correspond to peak periods in the range 5 to 7 s full-scale and 0.8 to 1.2 s at the 1:70th scale of these experiments. Since each experiment (e.g. a wake study) requires continuous wave- and current-generation for a period of several hours it is accepted that precisely calibrated wave conditions in the form of repeatable time-histories will not be possible. Generation of regular waves encountering a strong opposing current leads to a short crested wave-field of steep waves and reflections develop over the long intervals required to obtain velocity measurements at multiple points in the wake.

The approach taken is to develop a narrow-band irregular wave-field by allowing the development of reflections prior to commencing measurements. Testing indicates that it is not feasible to generate wave periods of less than 1 s on an opposing current of 0.45 m/s. A wave frequency of 0.8 Hz (T = 1.25 s) has been selected representing a period of approximately 10.5 s at full-scale (1:70th Froude Scaling). After continued generation for a period of several minutes, the wave conditions become irregular and considerably steeper. With an opposing current of 0.45 m/s a regular wave with frequency 0.8 Hz and amplitude of 10 mm (i.e. trough to crest height of 20 mm at experimental scale or 1.4 m at full-scale) develops into an irregular wave-field with significant wave height of approximately 50 mm (Figure 3.12). This is equivalent to a peak period of approximately 10.5 s and a significant wave height of 3.5 m. This irregular wave-field is short-crested hence the conditions measured vary slightly with measurement location. However, for a given period, a similar increase of wave height and change of spectral shape is observed for regular waves of larger amplitude (Figure 3.13).

As expected, the effect of imposed waves is to increase the total kinetic energy of the flow at frequencies close to the wave frequency (Figure 3.14). There is little change to the remainder of the energy spectrum of the flow.

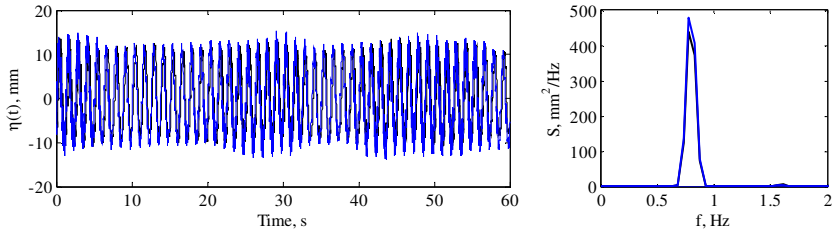

(a) Zero current. Measured $H_s \sim 22$ mm.

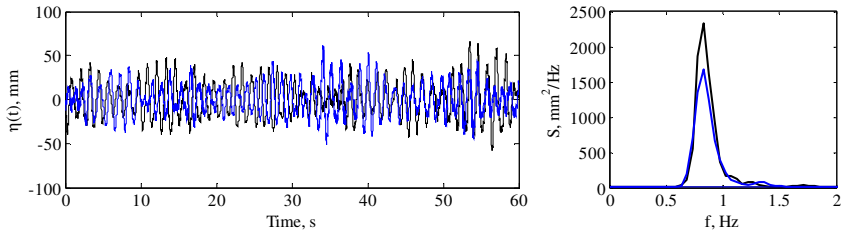

(b) Current of 0.45 m/s. Measured H_s ~ 50 mm

Figure 3.12: Surface elevation on centreline of flume at 1.8 m from paddles (Black) and at X = 9 m (Blue) corresponding to a location within the wake of an array. Measurements shown due to waves only (a) and waves generated on opposing current (b). Paddle motion specified to generate regular wave amplitude 10 mm and frequency 0.8 Hz with zero current.

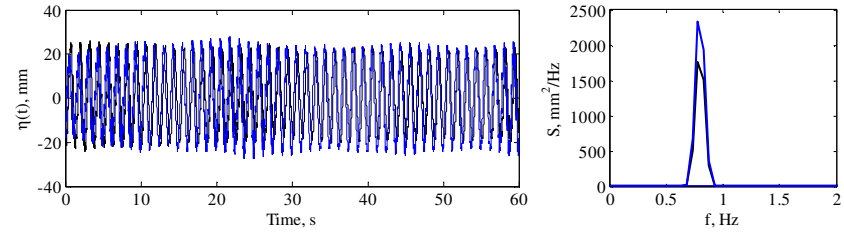

(a) Zero current. Measured H_s ~ 40 mm

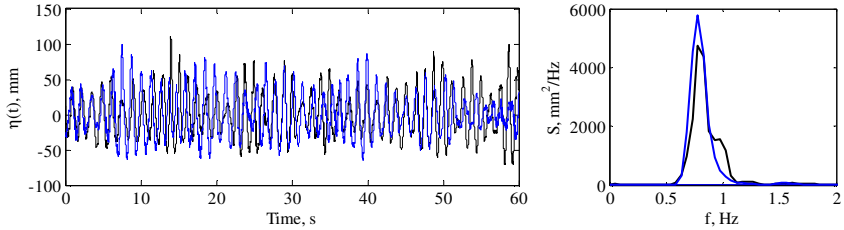

(b) Current of 0.45 m/s. Measured H_s ~ 80 mm.

Figure 3.13: Surface elevation on centreline of flume at 1.8 m from paddles (Black) and at X = 9 m (Blue) corresponding to a location within the wake of an array. Measurements shown due to waves only (top) and waves generated on opposing current. Paddle motion specified to generate regular wave amplitude 20 mm and frequency 0.8 Hz with zero current.

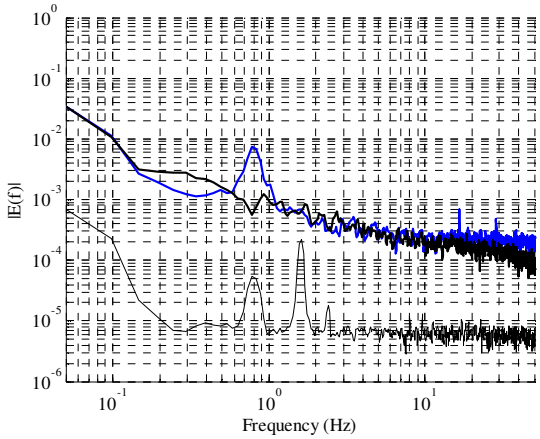

Figure 3.14: Spectrum of total kinetic energy for current only (thick black), for waves only (thin black, as for Figure 3.12(a)) and for current with opposing waves (thick blue, as for Figure 3.12 (b)). Velocity measured at x=9 m, y=2.483m, z=0.225m (channel centre, 1/2 depth)

The impact of the wave field upon the depth profile of the flow is illustrated in Figure

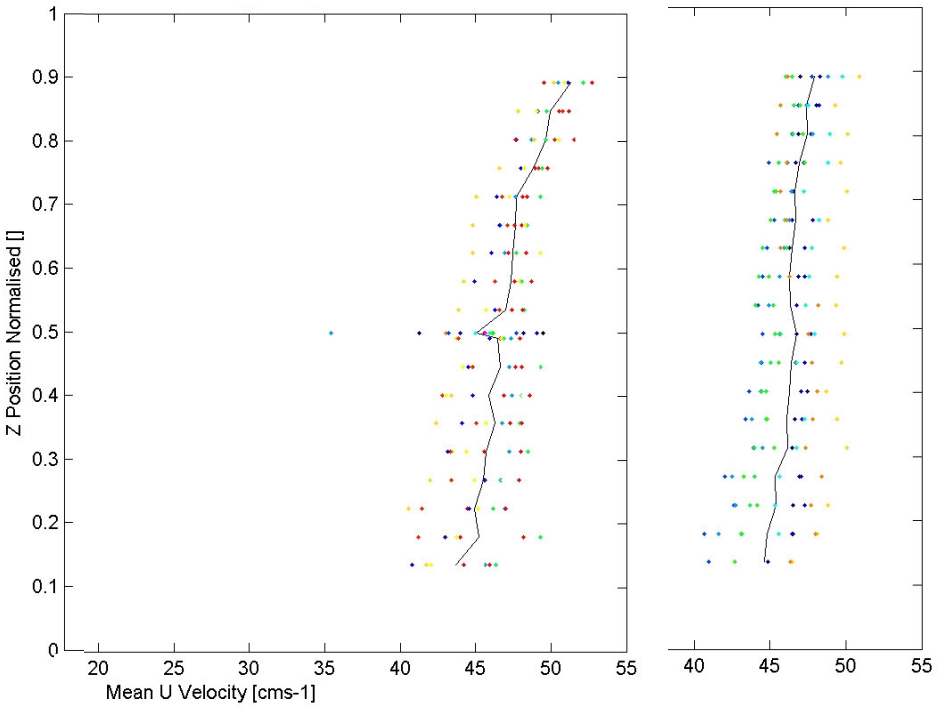

Figure 3.15: Depth-profile of axial velocity $U_x(z)$ at X = 7.5 m with and without a wave field (from left to right respectively).

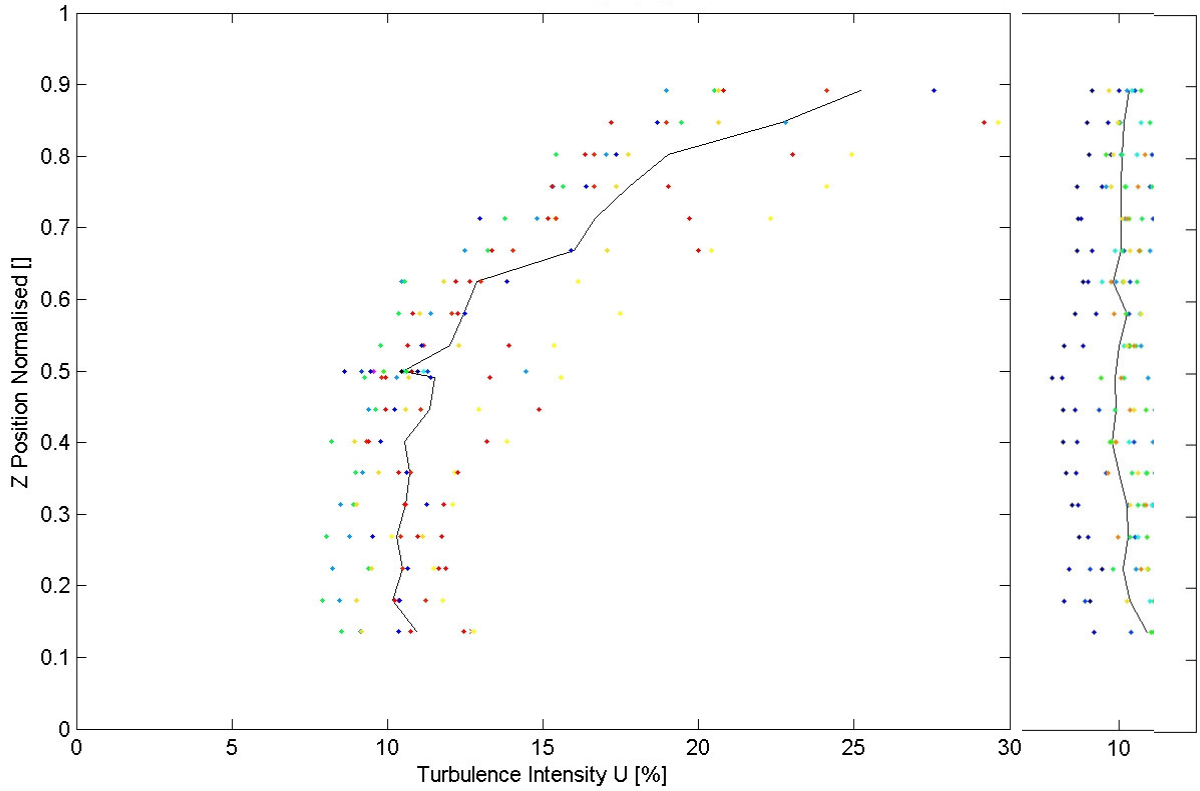

Figure 3.16: Depth-profile of turbulence intensity at X = 7.5 m with and without a wave field (from left to right respectively).

3.5 Large-scale Turbulent Structures: Conical Island

Large scale eddies are another source of turbulence which have the potential to introduce additional energy to the wake, potentially further aiding recovery. Section 2.4 and Appendix B of WG4WP2 D2 detail the geometry of a flat-topped conical island for developing large-eddy structures in the 0.45 m depth channel employed. The frustrum cone island has the following dimensions: Height = 0.4 m, base diameter = 1.6 m, top diameter = 0.4 m and mid-height diameter = 1.0 m. Analysis of velocity measurements of 10 minute duration (120000 samples) indicates the presence of periodic vortex shedding with a frequency of 0.138 Hz. Based on the diameter at mid-depth, this corresponds to a Strouhal number St ~ 0.31 (where St ~ fD/U = 0.138 * 1.0 / 0.44).

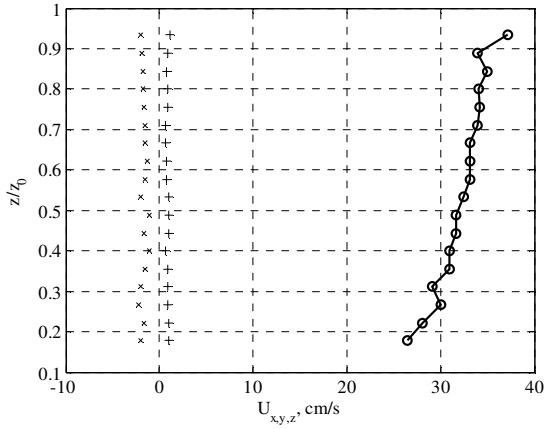

Figure 3.17: Depth profile of mean longitudinal velocity Ux (o), vertical velocity (+) and lateral velocity Uy (x) at mid-depth and centreline of flume. Global co-ordinate of measurement position (X, Y, Z) = (9000, 2500, 225) and island centre at (X, Y) = (5000, 2500).

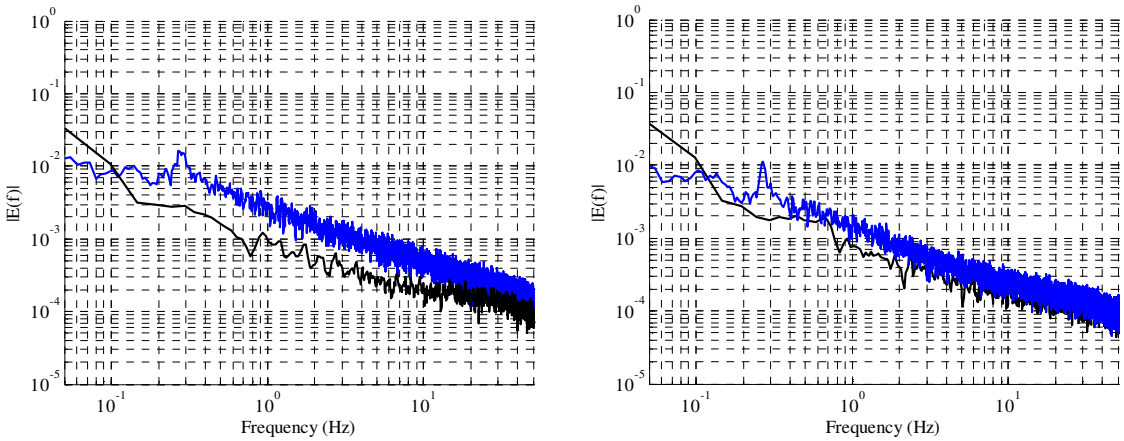

Figure 3.18: Spectrum of total kinetic energy at mid-depth on centreline of flume at X = 6000 mm (Left) and X = 9000 mm (Right). Island centre at (X, Y) = (5000, 2500). Spectrum of baseflow at the same measurement position also shown (thin black curve) for comparison.

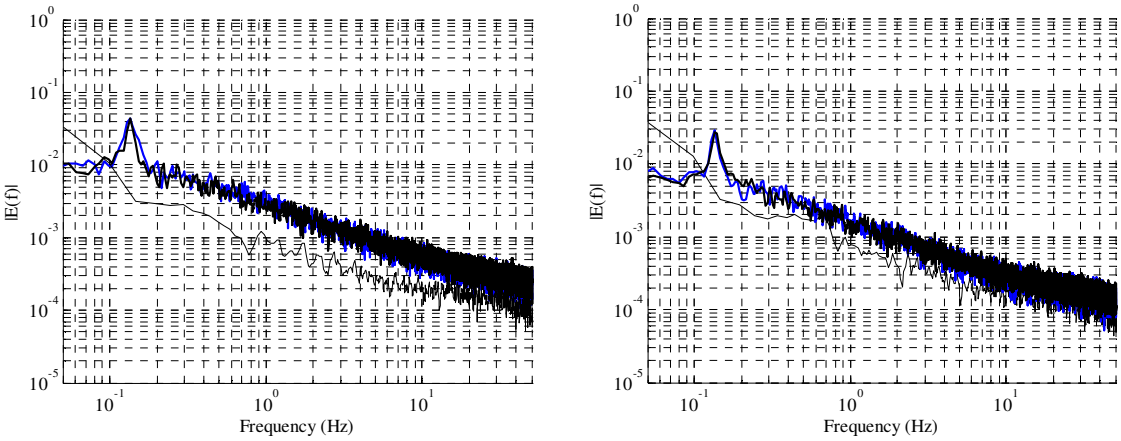

Figure 3.19: Spectrum of total kinetic energy at mid-depth at positions 500 mm either side of centreline of flume at X = 6000 mm (Left) and X = 9000 mm (Right). Spectra correspond to Y = +500 mm (thick black curve) and Y = -500 mm (thin black curve), spectrum of incident flow at mid-depth and mid-section also shown (thin black curve) for comparison.

4 TURBINE DYNAMOMETER & SUPPORT STRUCTURE

Each CROUZET dynamometer is referred to by a reference number PerAWaTXX where XX is a two digit integer value between 01 and 16. PerAWaT01 to PerAWaT03 were manufactured with two component strain gauges to allow measurement of axial force F_x (thrust) and transverse force F_y. PerAWaT04 to PerAWaT16 were specified with a single component strain gauge to provide measurement of axial thrust only. Unfortunately PerAWaT02 was not successfully calibrated and has since been rebuilt as a support structure with single component strain gauge. For each CROUZET dynamometer there are four calibration stages:

1) Calibration of strain gauges for Fx (all units) and Fy (units 1 to 3 only)
2) Measurement of tower load
3) Obtain torque constant of the CROUZET motor
4) Conduct rotor tests to obtain Igen and Ifric for specified tip speed ratio.

4.1 Strain Gauge Calibration

Strain gauges are calibrated by mounting the top-plate of the dynamometer vertically such that the tower is horizontal. Fixed increments of load are applied directly to the hub and the corresponding voltage recorded. The average voltage is subsequently obtained for each load increment and a linear relationship obtained between applied load and measured voltage by least-squares-best-fit. An example set of calibration data for the two strain gauges of PerAWaT01 is shown in Figure x.x. For each strain gauge a linear calibration constant is obtained such that $F_{x,y} = C(V) + V_0$. For F_x of PerAWaT01 C = -18.56 and V_0 = 2.910. Calibration constants for the first six dynamometers are listed in Table x.x. Note that, since the calibration is conducted with the support tower horizontal, the offset V_0 includes the self-weight of the tower. This tower self weight is not relevant during a test and so a test-specific zero offset is recorded for all strain gauges prior to each experiment. This is simply the average voltage measured when all support structures and rotors have been installed in still-water. This data is referred to as 'noflowhanging.dat'.

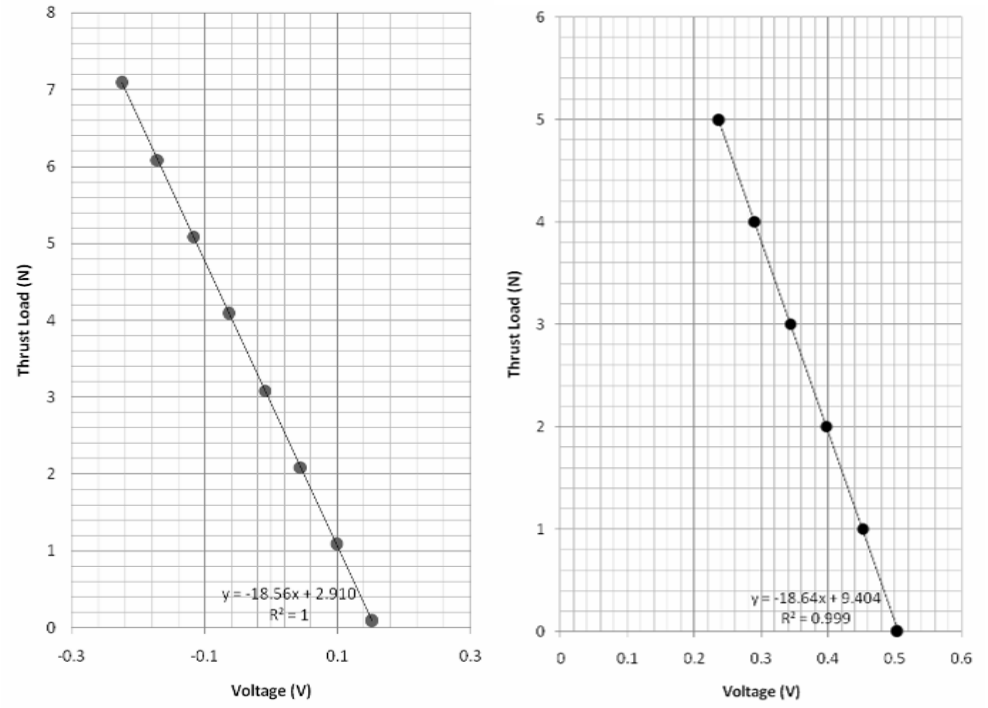

Figure 4.1**:** Calibration of strain gauge voltage output against increments of applied force at hub. Data and linear least-squares best-fit for in-line (F_x, left) and transverse (F_y, right) strain gauges of PerAWAT01. Note least squares residual R^2 ~ 1. See Table 1 for other dynamometers.

4.2 Tower load

Horizontal load measured by the strain gauges is due to horizontal thrust on the swept area of the rotor (approximately $F_{Rotor} \sim \frac{1}{2}C_T\rho A_D U^2$) and drag on the supporting shaft (approximately $F_{Drag} \sim \frac{1}{2}C_D\rho BLU^2$ where shaft width $B \sim 15$ mm, immersed length L ~ 22.5 cm). In WG4 WP2 D2, it was estimated that, for a flow speed of 0.5 m/s, rotor thrust is approximately an order of magnitude larger than the drag on the supporting shaft ($F_{Rotor} \sim 3$N, $F_{Drag} \sim 0.3$N). Measurements of the force on the CROUZET support structure only, i.e. without rotor attached, over a range of flow speeds indicate a maximum force on the supporting shaft of 0.26 N. This compares with a total horizontal force of the order of 5 to 6 N (see Section 5.1) so confirming that support structure loading is an order of magnitude smaller than the rotor thrust. The use of tower load as a variable

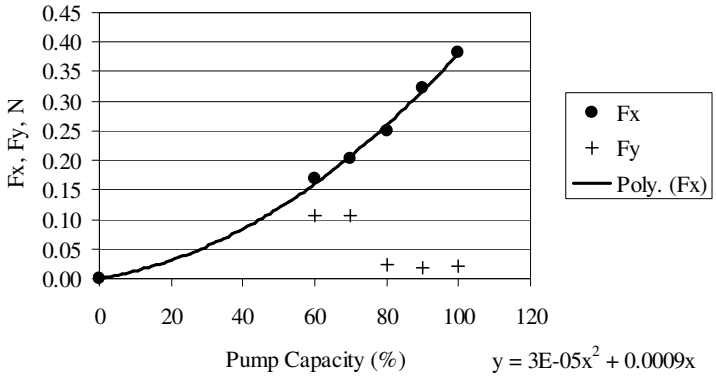

Figure 4.2: Variation of tower load for dynamometer PerAWaT03 expressed as equivalent longitudinal force (Fx) and transverse force (Fy) with pump capacity. Pump capacity is proportional to mean flow speed. Pump capacity of 100% corresponds to the baseflow conditions detailed in Section 3.3. Best-fit quadratic also shown indicating trend.

4.3 Torque constant for CROUZET motors

For each motor the torque constant has been calibrated by measuring the mean DC voltage induced in the motor whilst the motor is driven at a constant measured speed. Voltage is measured for a range of defined speeds to obtain a linear relationship between voltage and angular speed (Vs/rad) and, hence, of torque per Amp (Nm/A). Torque constant is obtained to an accuracy of less than 0.5%. Details of the calibration process and equipment employed are given by Brown (2009).

4.4 Torque-Speed Control

The rotor tests employ a constant torque control strategy (see WG4WP2D2) over a range of tip speed ratios. A torque control system is used that has been developed at UoM for experimental study of marine energy systems (details are given by Brown, 2009). The control system applies an assisting current I_A to provide a torque $T_m = I_A kT$ where kT is a torque constant with a unique value for each motor. We assign the following forms of the assisting current:

I_{Fric} is the assist current applied to compensate for mechanical friction in the system.

I_{Gen} is the assist current equivalent to the required (constant) torque when rotational speed is greater than ω_{min}. $I_{Gen} = \tau_m/kT$ where $\tau_m = P/\omega_{max}$.

I_A is the net assist current actually drawn by the drive. This is a function of I_{Gen} and shaft velocity (ω_d) as illustrated in Figure 4.3 and described below:

(1) If $\omega_d < \omega_{min}$, $I_A = I_{Gen}\omega_d/\omega_{min} + I_{Fric} = (\tau_m\omega_d/\omega_{min} - \tau_f)/kT$

(2) If $\omega_{min} < \omega_d < \omega_{max}$, $I_A = I_{Gen} + I_{Fric} = (\tau_m - \tau_f)/kT$

(3) If $\omega_{max} < \omega_d$, $I_A = I_{Gen}\omega_{max}/\omega_d + I_{Fric} = (T_m\omega_{max}/\omega_d - T_f)/kT$

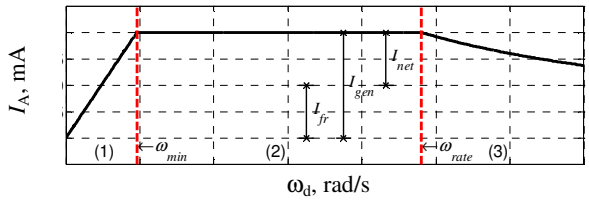

Figure 4.3: Static characteristic specified in firmware controller.

Both I_{Fric} and I_{Gen} are specified prior to each test. I_{Fric} is typically negative and I_{Gen} is always positive. Thus, whilst shaft speed is low, the assisting current is –ve and sufficient to compensate for mechanical friction in the system. As rotational speed increases due to rotor loading the assisting current is increased as a linear function of speed until the net torque due to both the drive and the friction in the system is equivalent to the required (constant) torque. For all shaft speeds between ω_{min} and ω_{max}, the assisting current is given as I_{Gen} + I_{Fric} only; i.e. constant torque. If the shaft speed exceeds the rated speed, the assisting current is reduced to avoid overloading the motor. Two variables are measured: angular speed (ω) and the applied current (I_A) which is reported to Labview as a voltage that is proportional to the bridge current across the motor. The relationship between instantaneous current, IA (mA) and Voltage output by the dynamometer controller is specified as I_A = 100(Volts) – 250. Calibration indicates that the average relationship for dynamometers calibrated to date is IA = 105(Volts) – 265. This small offset is due to the length of cable (~10 m) between dynamometer and logging system.

Angular speed (ω) is defined as the rate of change of angular position. Position is measured using a HEDS 9000 quadrature encoder reading an HEDM 6120 T12 code wheel. These codewheels provide 2000 counts per revolution. A brief calibration of each codewheel has been conducted by rotating through +360° and subsequently –360° to confirm that net zero count is returned. No further calibration is conducted of these components. The torque controller determines speed at 20 Hz increments and so speed is obtained to within 0.5%. For data logging purposes, angular position is sampled at 200 Hz and the accuracy of speed is therefore considerably higher. For these tests the rotor radius is 0.135 m and flow velocity is 0.45 m/s. Tip speed ratios in the range 2 < TSR < 10 are required and so the operating range of the torque-controller are specified as ω_{min} = 5 rad/s and ω_{max} = 30 rad/s. This control method provides a constant torque during an unsteady inflow (e.g. Figure 4.4).

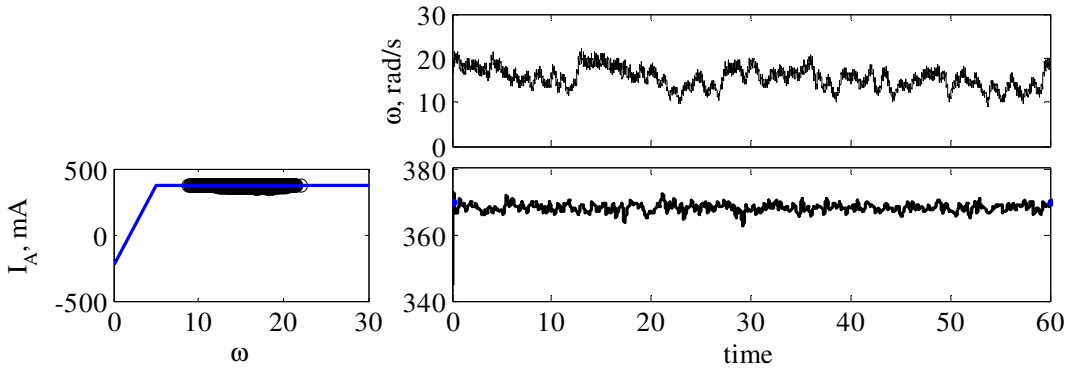

Figure 4.4: Time variation of torque (bottom) corresponding to time-varying angular velocity (top) due to unsteady incident flow with mean velocity of 0.45 m/s, Igen = 600 mA, Ifric = -130 mA. Measured torque and speed (black markers) compared to target torque-speed characteristic (blue curve, bottom left).

4.5 Summary

Strain gauges are calibrated by measurement of output voltage for several increments of applied force. This provides a linear calibration constant that is unique to each strain gauge. The variation of tower load with flow speed has been obtained prior to installation of the rotor and found to be small relative to thrust on the rotor. The torque control system has been calibrated and it is demonstrated that constant torque is maintained whilst incident flow velocity and rotational speed fluctuate. Relevant calibration parameters are given for the first six dynamometers in Table 1. The same procedures will be applied to further dynamometers immediately prior to their use to ensure that calibrated parameters are relevant to the corresponding test. For all tests, relevant calibration parameters are recorded in a "readme" file which also details the configuration of all equipment. Data files, corresponding readme files and calibration files for the tests completed to-date are stored in a database on the GH ftp site.

Table 1: Calibration constants for dynamometers PerAWaT01 to PerAWaT06

		Dynamometer Number: PerAWaTxx						
		01	03	02	04	05	06	07-15
FORCES								Prior to each test
Fx constant	N/V	-18.56	17.840	9.523	9.449	-9.160	-8.438	
Fy constant	N/V	18.64	-17.36	n/a	n/a	n/a	n/a	
TORQUES								
Motor No.	-	01	03	02	04	05	06	
Torque const.	Nm/A	0.0786	0.0793	0.07812	0.0784	0.0783	0.0787	
Friction torque	Nm							

Note: These values are correct at the time of writing but values given in the readme file corresponding to a specific set of data should always be used for data analysis.

5 DEVICE BASELINE DATA

A 3-bladed rotor of 0.27 m diameter has been designed using GH Tidal Bladed (Section 7 of WG4 WP2 D2). This small-scale rotor was designed to develop a similar relationship between thrust and rotational speed as a generic full-scale turbine – i.e. to produce a similar CT(TSR) curve to a full-scale turbine. After preliminary testing, the rotor geometry defined in Appendix E of WG4 WP2 D2 was modified close to the root (WG4 WP2 D3) and manufactured by the rapid prototyping method SLS from glass fibre reinforced polymer-acrylic (PA12-GF).

The characteristic of this rotor – specifically the relationship between thrust and rotational speed – informs all further tests. Multiple tests have therefore been conducted to determine the CT(TSR) curve. For a single dynamometer the procedure is:

1) Set I_{Fric} to a nominal value which compensates for most of the friction in the system.
2) Measure thrust and TSR for a range of IGen values (100 < IGen < 999 mA). This provides the rotor characteristic as discussed in Section 5.1.

Subsequently, this data is employed to select the torque value required to obtain a TSR value for each wake study. For a test comprising multiple dynamometers the following steps are first conducted for each dynamometer:

3) Select IGen corresponding to the TSR value of interest.
4) Confirm predicted rotor TSR by measuring CT(TSR) for dynamometer in isolation
5) Conduct wake measurements as discussed in Section 5.2.

These stages and corresponding measurements are summarised in the following sections.

5.1 Rotor Characteristic

Time variation of incident flow velocity, rotor loading and rotational speed has been obtained for multiple increments of applied torque. The inflow conditions of Section 3.3 are employed for the data reported in this section. A sample of the incident flow is shown in Figure 5.1 in addition to the corresponding angular speed, which tends to fluctuate during and the constant torque applied during the test. The corresponding time-history of axial and traverse force is shown in Figure 5.2. Clearly the transverse fluctuates but is very small magnitude and with a mean close to zero so can be neglected. The axial force also fluctuates, due to variation of angular speed.

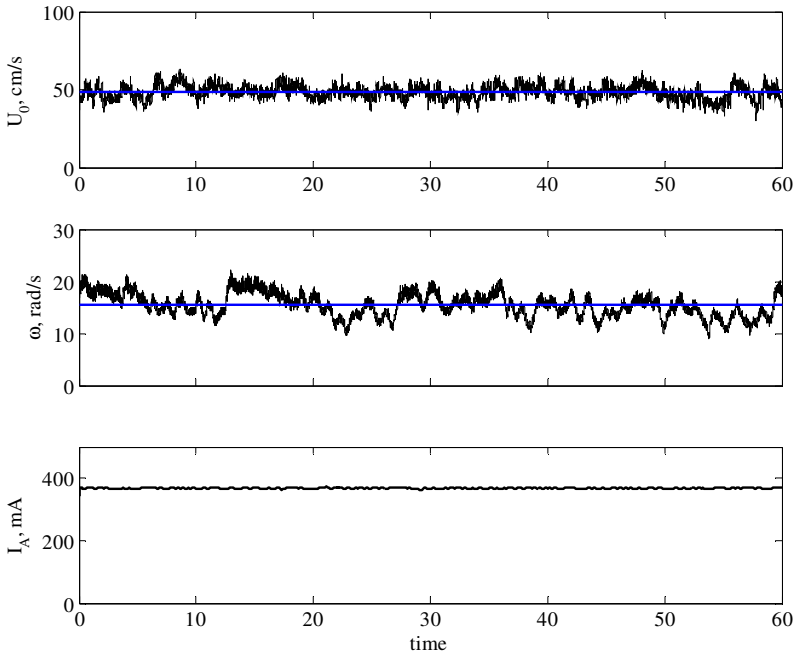

Figure 5.1: Time history of incident flow velocity U(t), angular speed and instantaneous current. Corresponding time history of loading shown in Figure 5.2.

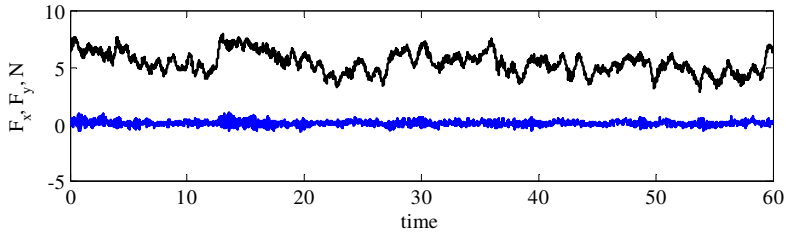

Figure 5.2: Time history of thrust force (Fx) and transverse force (Fy). Thrust force reduced by tower load (see Section 3.2 and text prior to)

Analysis of time-histories for multiple increments of applied torque provides the relationship between thrust coefficient and tip speed ratio. A comparison of the predicted CT(TSR) and CT(TSR) measured using two dynamometers is given in Figure 5.3 indicating reasonable agreement with predictions. Measurements are shown for two cases. The total force due to flow-induced load on both the rotor and the tower is consistently higher than the predicted values of CT. High values of CT are partly due to the loading on the tower and so CT for the rotor alone is estimated by subtracting the tower load measured due to incident flow alone (see Section 4.2). Of course this is an approximation since the flow velocity on the tower will differ due to the rotor wake. Alternative estimates of the tower loading could be modified based on estimates of the reduced velocity in the wake and the change of bypass flow velocity but this is not expected to significantly alter the tower load and so such analysis is not considered at this stage.

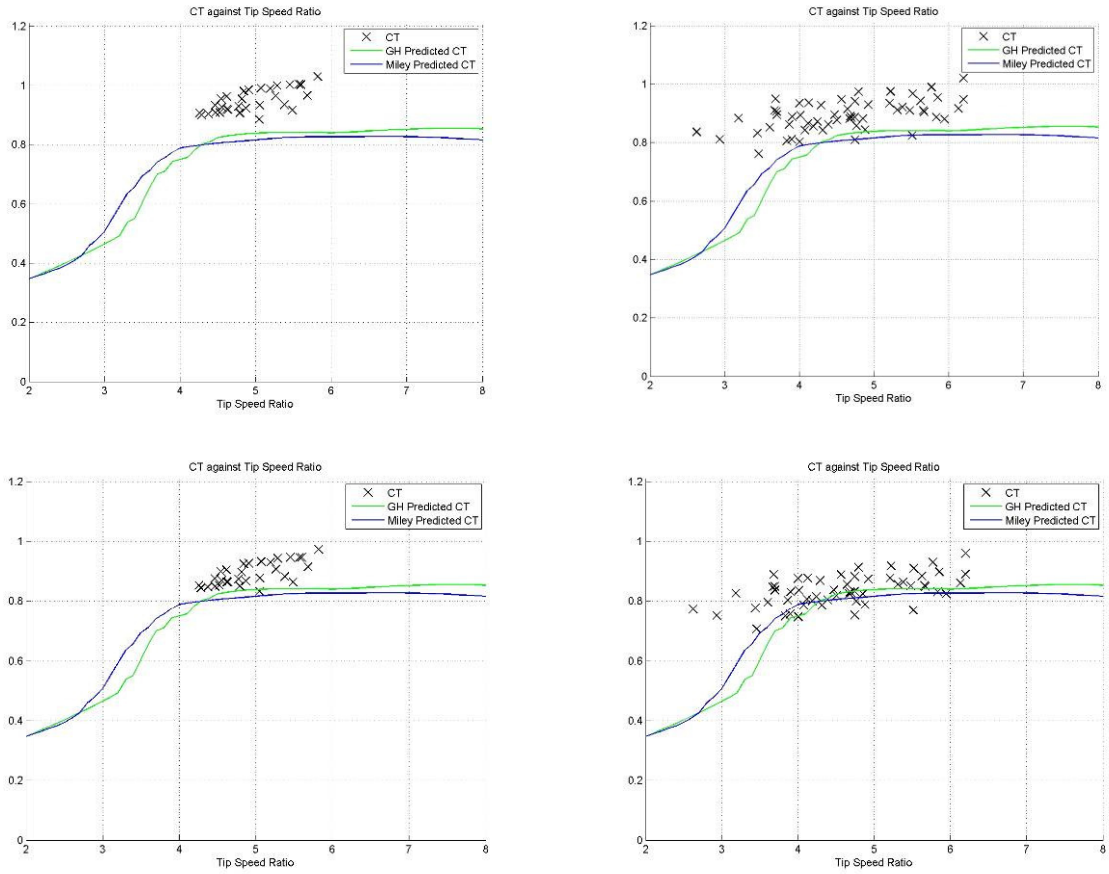

PerAWaT01 PerAWaT03

Figure 5.3: Measured CT(TSR) compared to BEM Predictions (see WG4WP2D2 for details of GL-GH predicted CT). Thrust coefficient shown including tower drag (top) and after removal of tower drag (bottom).

5.2 Wake Structure

Having identified the performance characteristics of a single rotor, the structure of the wake of a single rotor has been measured to provide a baseline for assessing the effect of lateral spacing on wake structure. This study comprises a longitudinal profile of 12 ordinates over the range 1.5D < X < 20D downstream of the rotor plane and vertical and transverse profiles across the width of the wake and depth of the flow at increments of 10 mm. This comprises 180 velocity measurements of 60 s duration sampled at 200 Hz. The measurement co-ordinates are illustrated in Figure 5.4. An appropriate Igen value has been obtained based on the CT(TSR) characterisation study. Measurements of CT(TSR) during the wake study are shown in Figure 5.5 indicating that the process of identifying torque provides a representative TSR within the variation that occurs due to the performance of the rotor in turbulent flow.

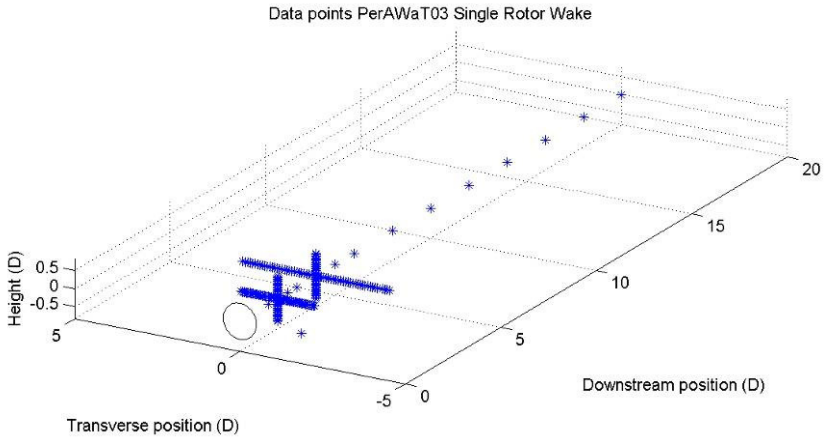

Figure 5.4: Data collection points for single wake study.

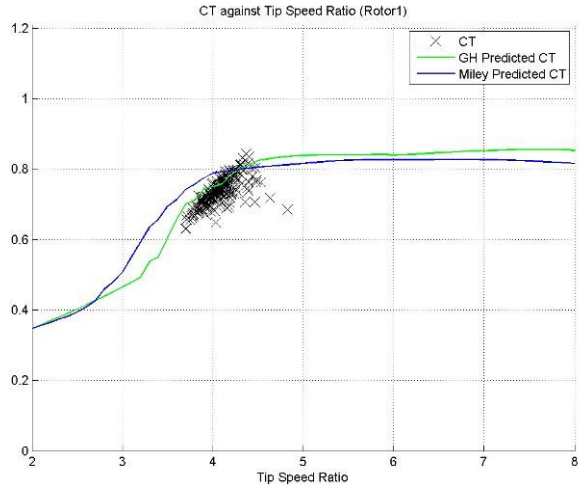

Figure 5.5: CT vs TSR measured during study of single wake

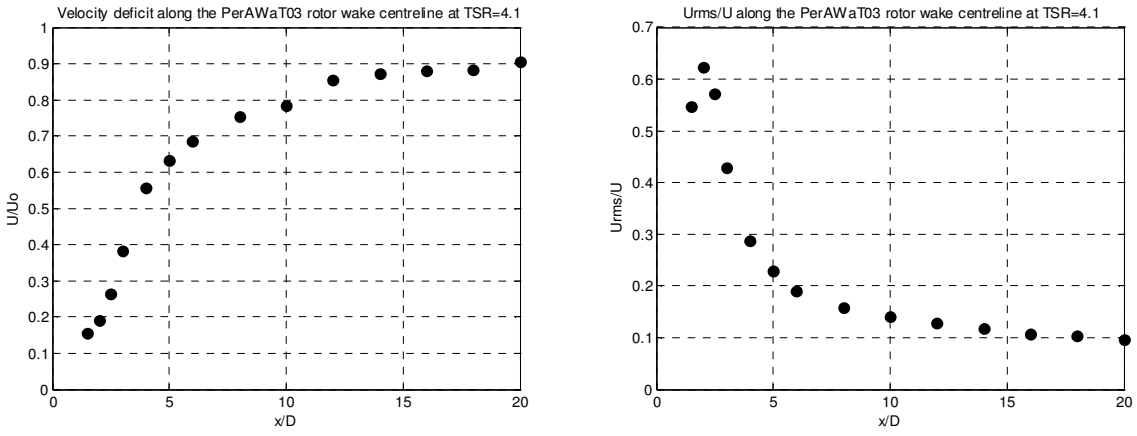

Figure 5.6: Axial velocity (U/U_0 left) and relative turbulence intensity (Urms/U) along centreline of wake over range 1.5 D < x < 20 D. Average TSR = 4.1 and average thrust coefficient CT = 0.76 (see Figure 5.5)

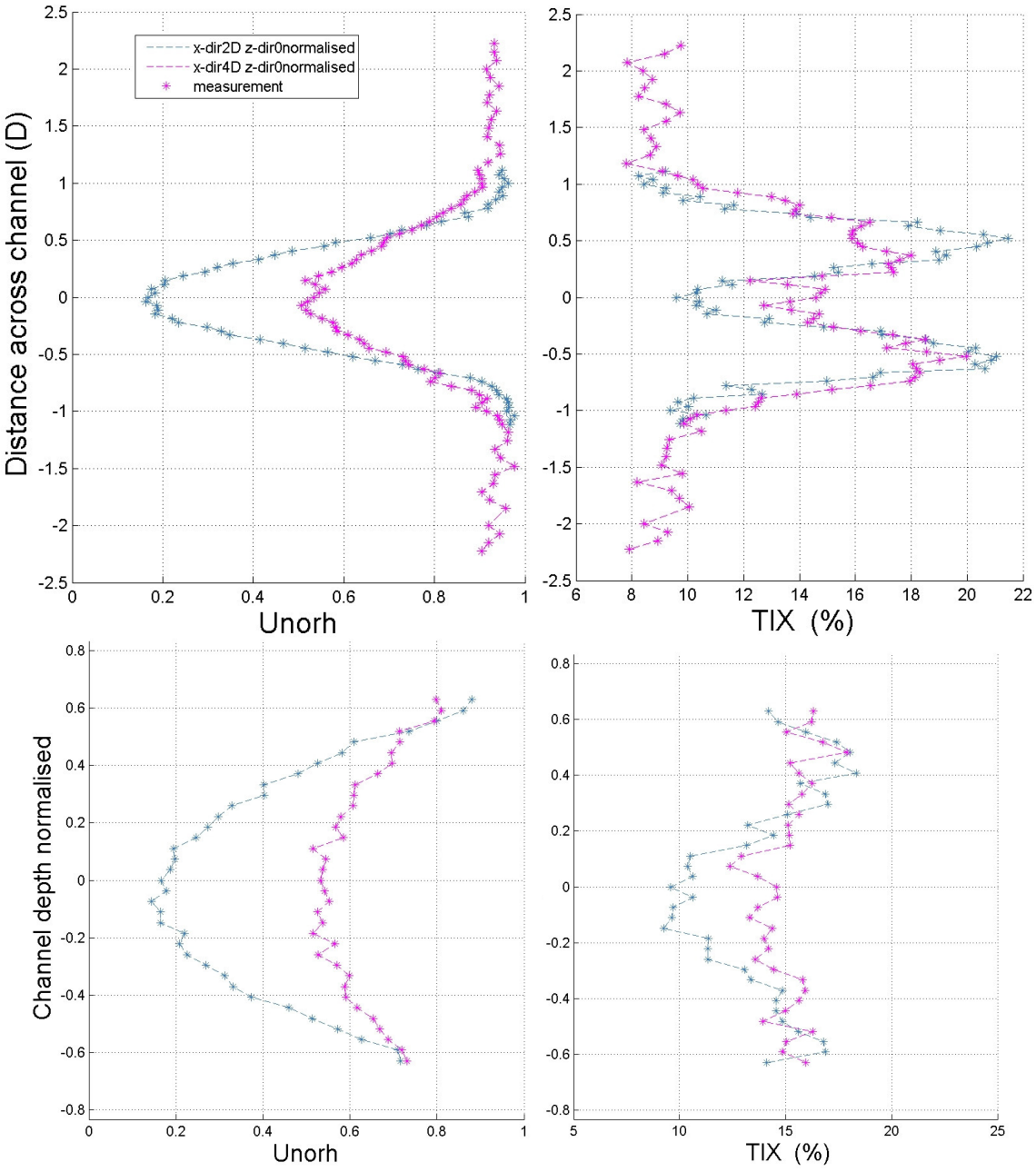

Figure 5.7: Lateral (top) and vertical (bottom) profiles of axial velocity (Unorh) (left) and Turbulence Intensity (TIx) (right) for cross sections of the wake at 2D and 4D downstream. Average TSR = 4.1 and average thrust coefficient CT = 0.76 (see Figure 5.5). Water depth = 0.45 m and hub at mid-depth.

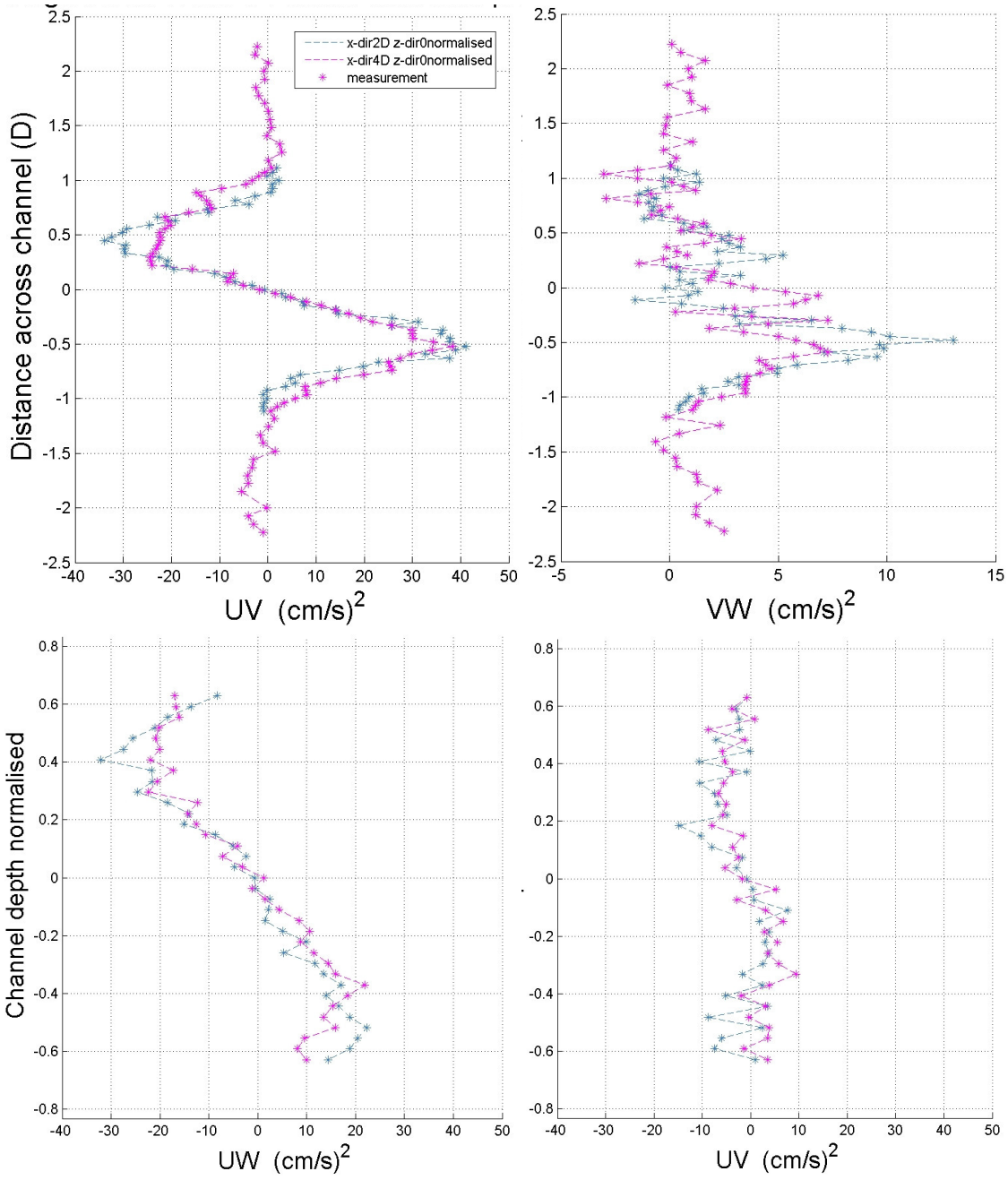

Figure 5.8: Lateral (top) and vertical (bottom) profiles of normalised Reynolds Stresses for cross sections of the wake at 2D and 4D downstream. Average TSR = 4.1 and average thrust coefficient CT = 0.76 (see Figure 5.5). Water depth = 0.45 m and hub at mid-depth.

When normalised to the baseflow profile (see Section 3.3) it is clear that the wake structure of an isolated device is axisymmetric (Figure 5.9).

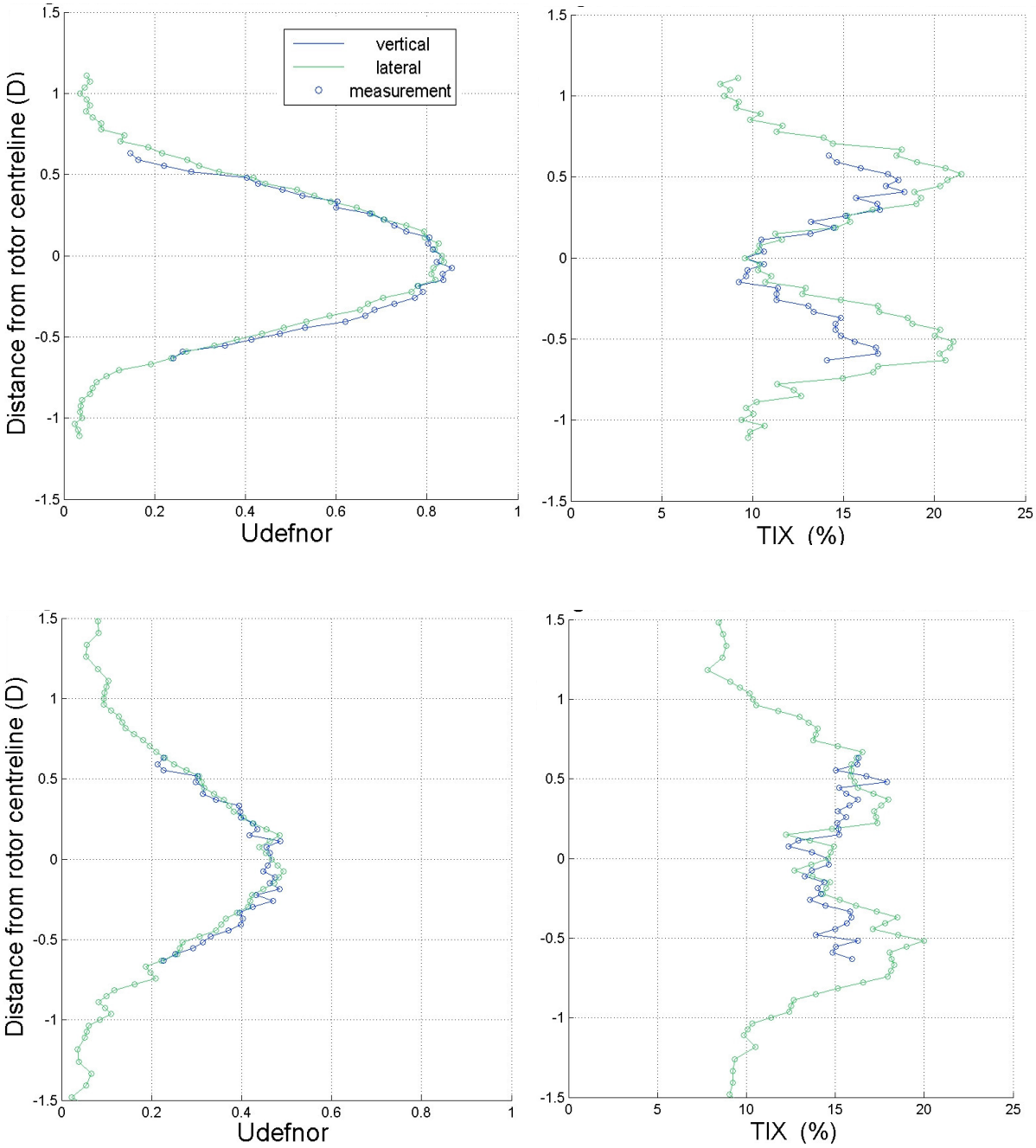

Figure 5.9: Comparison of vertical and lateral profile of velocity deficit (left) and turbulence intensity (right) at 2D (top) and 4D (bottom) downstream of a single rotor.

5.3 Two devices (lateral blockage)

The foregoing sections demonstrate that all equipment has been calibrated and that the structure of both the ambient flow and wake of a single device has been obtained. Measurements of the wake of two devices have recently been completed at 1.5D spacing, 2D spacing and 3D spacing. These tests represent the first stage of the investigation of lateral blockage on rotor loading and wake recovery. Initial analysis of the wake of two rotors at 1.5 D lateral spacing is given in Figures 5.10 and 5.11.

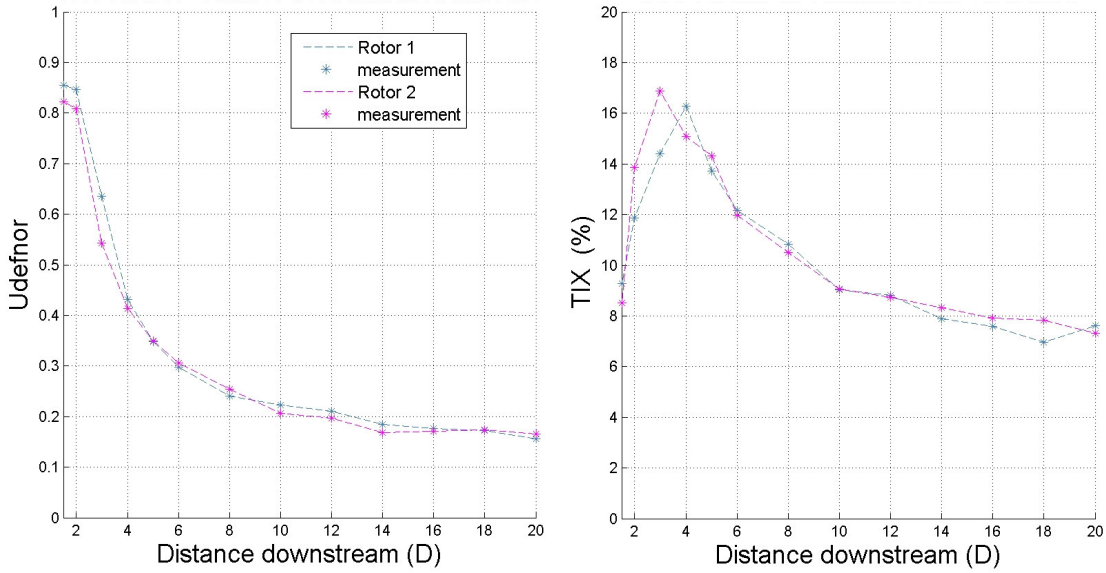

Figure 5.10: Axial velocity deficit (left) and turbulence intensity (right) along centreline of wake over range 1.5 D < x < 20 D.

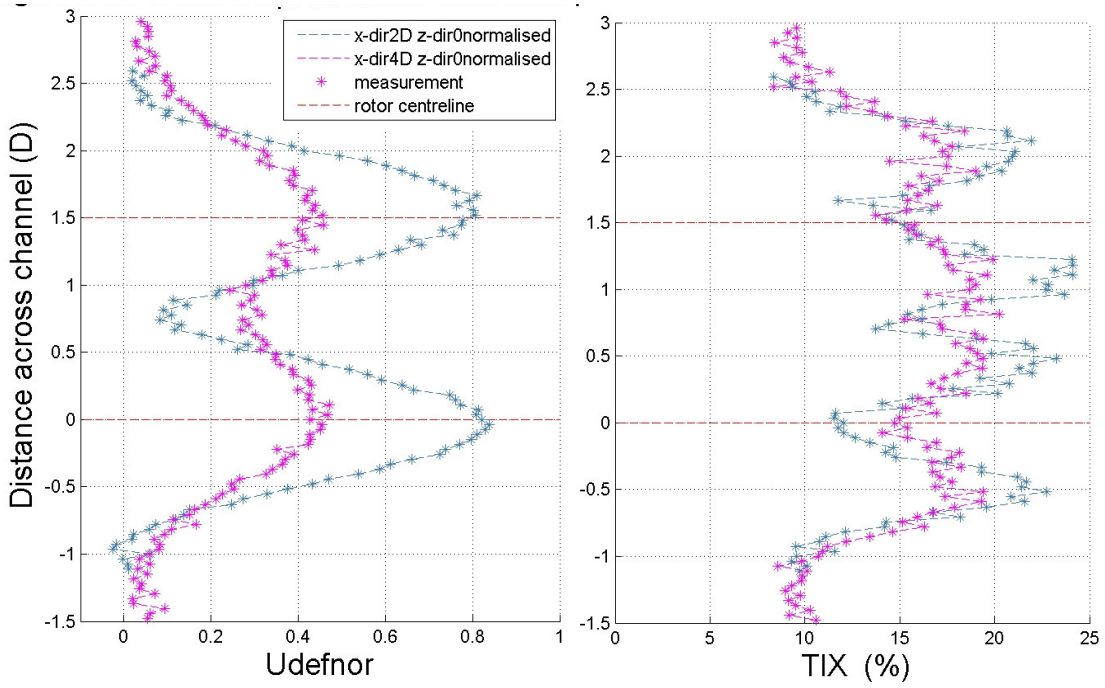

Figure 5.11: Lateral profile of velocity deficit (left) and turbulence intensity (right) in the wake at 2D and 4D downstream of two rotors.

6 DATABASE

All data collected as part of the WG4WP1D4&D5 will be collated within a database as required by the PerAWaT project. The list of planned experiments and range of measurement positions is given in Appendix B. Experiments 1 to 5 of that list have been executed as part of D4 to provide calibration data of the baseflow, rotor characteristics and of a single and dual rotor wake map. The data generated by the experiments has been processed by GH and collated with a database and is available to view on the ftp server (ETI@ftp.garradhassan.com) within the folder structure: *Tidal/Deliverables/WG4 WP2 D02/GH Data Processing/2011.* A description of the available data contained within the database are detailed below:

Input data per experiment

- "Readme" file including
  - Location of each rotor
  - Location and orientation of each ADV provided via ADV.dat file name
  - Calibration parameters for axial force, rotor torque and, if necessary, wave gauges
  - Explanation of column arrangement of raw data files.
- Data recorded prior to test for baseline:
  - COR & SNR for all ADVs in test configuration
  - 'noflowhanging.dat' as per raw data files but measured with zero flow velocity.
- Raw data files. Separate file for each flow-co-ordinate. Data sampled at 200Hz and including the following:
  - ADV velocity measurement (4 components per ADV) for ADVs downstream of rotors
  - ADV velocity measurement at upstream location for evaluation of CT &CP
  - Strain gauges measurements i.e. to obtain axial force per rotor
  - Angular position per rotor i.e. to obtain angular angular velocity per rotor
  - Dynamometer motor current measurement i.e. rotor torque per rotor

Processed data per experiment

- Location of rotors and measurement points
- Reference inflow mean flow speed
- Mean Ct per rotor per experiment

Processed data plots per experiment

- Spatial location of data points
- Baseflow profile used to normalise velocity data
- CT vs TSR for each rotor
- COR & SNR time histories
- Flow field plots including:
  - Mean velocity (U,V,W)*
  - Turbulence intensity (U,V,W)*
  - Reynolds Stresses (XY,YZ,ZX planes)
  - Kurtosis
  - Skewness
  - Turbulent Kinetic Energy

  For each of the above parameters the following plots are produced
  - Lateral profiles
  - Vertical profiles
  - Centreline profiles
  - Lateral profiles vs vertical profiles
  - Surf and contour plots if required

*** Suffixes**

X = in the axial direction

Y = in the transverse direction

Z = in the vertical direction
def = The deficit of the plotted parameter when compared to ambient flow
nor = values normalised against ambient flow data
norh = values normalised against the hub height value of ambient flow data

7 SUMMARY

This report provides a summary of the key calibration tests for the flow-conditions and experimental equipment used for the small-scale tidal stream turbine array tests of WG4 WP2. An explanation is given of the calibration procedures and examples of key parameters are given. The information presented demonstrates that the required rotor tests can be calibrated correctly such that the measured data will satisfy the specification given in WG4 WP2 D1.

Ambient flow conditions with a mean velocity of 0.45 m/s have been measured at three cross sections of the flow corresponding to the plane of the first row of rotors (X = 6 m from the inflow weir) and to sections within the wake. The incident flow velocity varies by less than 3 cm/s over the width of the arrays to be studied. Turbulence intensity is approximately 10% over the same width although decays to approximately 8% between X=6 m and X=9 m. Since this distance is more than 10 D, this small decay of turbulence intensity is acceptable.

Wave conditions opposing the direction of current flow have been investigated. The selected conditions correspond to a short-crested narrow band wave-field with peak frequency 0.8 Hz and significant wave height of approximately 50 mm. Applying Froude scaling these conditions correspond to full-scale wave conditions with peak period 10.5 s and significant wave height 3.5 m. These irregular waves are generated by imposing a periodic paddle motion that in the absence of current generates a regular wave only. After continued interaction with an opposing current of 0.45 m/s, the short-crested irregular wave-field develops. These wave conditions represent a considerable increase of vertical forcing across the wake region and so are considered suitable for assessing the effect of waves on wake recovery. Ambient flow conditions with significantly higher lateral forcing are developed due to the oscillatory flow downstream of a conical island. Preliminary analysis of this flow indicates a shedding frequency from the island of St ~ 0.31. This is marginally higher than the value 0.28 suggested in WG4WP2D2 but considered suitable for representing the effect of large-scale turbulent structures on wake recovery. The final flow condition of increased turbulence due to a rough-bed has not yet been studied in detail. Installation would interrupt the planned schedule of wake studies and so priority has been given to the rotor array studies. After installation, the flow due to the rough bed material will be measured at the same sections as the incident flow (Section 3) and the array reinstalled after calibration of the flow.

Processes are described for calibration of all measurement devices for the principal variables of interest. These include strain gauges and the speed-torque measurement system for each dynamometer. At the time of writing, not all equipment has been calibrated but the processes described in this report are relevant to all items of equipment. Specifically, not all strain gauges have been calibrated since it is logical to calibrate immediately prior to each test. To-date, tests have been conducted with up to three dynamometers and so further strain gauges will be calibrated when the dynamometer is required. Similarly, tower load has been measured for the dynamometers that have been used and will be measured for additional dynamometers immediately prior to use.

To evaluate the effects of blockage and different ambient flow conditions on rotor performance and wake structure investigations have been conducted of the rotor characteristic (in terms of CT(TSR)) and of the wake of a single rotor. Measurements of CT(TSR) are reported for two different dynamometers (PerAWaT01 and PerAWaT03) over the range $3.5 < TSR < 7$. Measurements are shown to be repeatable with different equipment. For a given TSR, thrust is higher than the BEM predictions detailed in WG4WP2D2. As noted in WG4WP2D2 this is not unexpected and can be attributed to several factors including the assumptions of the BEM calculation method used, the accuracy of CD, CL data and the effect of free surface proximity. Predictions are based on CD and CL data for a 2D blade section in uniform flow at similar Reynolds number (order of 30,000). Note that two sources of CD and CL data for the same blade section suggest approx 10% variation of thrust at

TSR close to 4. The variation of measured CT is therefore acceptable and provides a basis for evaluating the effect of lateral blockage and for specifying the dynamometer operating point for subsequent wake studies.

Measurements of a single rotor wake include a longitudinal profile along the axial centreline over the range 1.5D < X < 20D and both transverse and vertical profiles of the wake at 2D and 4D downstream of the rotor plane. The longitudinal profile demonstrates that velocity recovers to approx 95% of the free stream velocity at 20 diameters downstream. Lateral and vertical profiles can be made sufficiently close to the rotor plane to identify the start of the far wake. Measurements are of sufficient accuracy and resolution to provide meaningful profiles of turbulence intensity and Reynolds Stress. The measured velocity is normalised to the ambient flow. For this wake study, dynamometer torque was specified to obtain an average TSR of 3.5. The CT(TSR) recorded during each wake measurement (a total of more than 200 minutes of data sampled at 200 Hz) confirm that the average CT(TSR) during the wake study is consistent with the specified value of TSR.

Initial measurements are presented of a wake study comprising two devices at lateral spacing of 1.5D. This represents the simplest ‘array’ considered in this work package. Detailed analysis of this data is beyond the scope of this report but the plots presented demonstrate that the calibration data for both equipment and flow is sufficient for the planned array studies. Experimental measurements are now ongoing following an agreed schedule. Key stages include:

- Wake measurement of three devices on single row (ongoing)
- Wake measurement of two rows of three devices
- Wake measurement of three rows of three devices
- Modification of wakes due to increased vertical forcing (waves), lateral forcing (island) and due to increased turbulence (rough bed). This stage of work includes installation of rough bed material and flow-measurement prior to testing.
- Wake measurement of arrays of up to 15 devices

Note: Specific values are given in this report for various mechanical properties. These values are correct at the time of writing. However, any values may be superseded by values given in the readme file for a specific test. Values given in the readme file corresponding to a particular test should always be used for data analysis.

REFERENCES:

Brown (2009) Design and Construction of a Dynamometer System for Testing and Array of Wave Energy Point Absorbers. MPhil Thesis, University of Manchester.

APPENDIX A

In addition to the summary figures of velocity, turbulence intensity and cross-correlation shown in the report, additional moments of the data may also be of interest. Plots of the following parameters are also produced during data analysis and are included in the database on the GL-GarradHassan ftp site.

Second moment = mean-square departure from the time-averaged velocity = variance or mean square

$$\sigma^2{}_x = \overline{u^2}$$

The square root of the variance is the standard deviation

Skewness (S_x)

$$S_x = \frac{\overline{u^3}}{(\overline{u^2})^{3/2}}$$

Kurtosis or flatness factor or excess (K_x)

$$K_x = \frac{\overline{u^4}}{(\overline{u^2})^2} - 3$$

Longitudinal turbulent flux of TKE

$$TKEf_j = \rho \frac{\overline{q^2.u_j}}{2} \quad \text{for } j = x,y,z$$

Reynolds stresses

$$\bar{\tau}_{xx} = \bar{p} - \rho\overline{u^2} \qquad \bar{\tau}_{xy} = \mu\frac{\partial\overline{U}}{\partial y} - \rho\overline{uv} \qquad \bar{\tau}_{xz} = \mu\frac{\partial\overline{U}}{\partial z} - \rho\overline{uw}$$

$$\bar{\tau}_{yx} = \mu\frac{\partial\overline{V}}{\partial x} - \rho\overline{vu} \qquad \bar{\tau}_{yy} = \bar{p} - \rho\overline{v^2} \qquad \bar{\tau}_{yz} = \mu\frac{\partial\overline{V}}{\partial z} - \rho\overline{vw}$$

$$\bar{\tau}_{zx} = \mu\frac{\partial\overline{W}}{\partial x} - \rho\overline{wu} \qquad \bar{\tau}_{zy} = \mu\frac{\partial\overline{W}}{\partial y} - \rho\overline{wv} \qquad \bar{\tau}_{zz} = \bar{p} - \rho\overline{w^2}$$

For each term the first subscript indicates the normal to the surface on which the stress is acting and the second one indicates the direction of action. The Reynolds stress are those that occur from the cross correlation of orthogonal velocity components. Lateral $\bar{\tau}_{yx}$ and vertical $\bar{\tau}_{zx}$ Reynolds Stress are of interest. Note that the effect of molecular viscosity will be small e.g. mu = 10-4, and at max dU/dy <1 compared with the product of density and the fluctuation terms (of order of 0.01) so leading to the cross correlation term being dominant by several orders of magnitude.

APPENDIX B

Array configurations and corresponding velocity measurement positions. Each wake study comprises a longitudinal traverse of nX positions, a number nXPOS lateral traverses. Each lateral traverse comprises nY measurement positions and nXY(Z) depth profiles of nZ positions.

			Array Size		Array Configuration		VELOCITY DATA TO OBTAIN											
							CENTRELINE velocities (Diameter multiples)				TRAVERSES - U(Y) Wake width ~ 1.5 Diameters						Depth Profile - U(Z)	
			No. of ROTORS		Rotor Centre Spacing													
No.	REF	Description	min(N)	max(N)	Y-Space (D)	X-Space (D)	nX	Xmin	Xmax	nADV	nXPOS	XPOS	nY	Ymin	Ymax	nXY(Z)	nZ	
1	FLOW01	Baseflow	0	0														
2	FLOW02	Baseflow with waves	0	0														
3	FLOW03a	Baseflow with weir measured across test section	0	0						1	3	6, 7.5, 9	12	wall	wall	3	40	
3.1	FLOW03b	Baseflow with weir measured at 3 depths								3	3	6, 7.5, 9	12	wall	wall	9	40	
4	CT01	Rotor performance	1	1	n/a	n/a	1	2	n/a	1	1	1D	-	-	-	0	-	
4.1	CT02	Rotor performance repeat	1	1	n/a	n/a	1	2	n/a	1	1	1D	-	-	-	0	-	
4.2	CT03	Rotor performance with different torque applied	1	1	n/a	n/a	1	2	n/a	1	1	1D	-	-	-	0	-	
5	WAKE01	Single device wake	1	1	n/a	n/a	10	2	10	1	2	2D, 4D	40	-2	2	0	40	
6	WAKE02a	2 device, 1 row, 1.5D spacing (A)	2	2	1.5	n/a	10	2	10	1	2	2D, 4D	80	-1.5	3	2	40	
7	WAKE02b	2 device, 1 row, 2D spacing (B)	2	2	2	n/a	5	2	10	2	3	2D, 4D	80	-1.5	3.5	2	40	
8	WAKE02c	2 device, 1 row, 3D spacing (C)	2	2	3	n/a	5	2	10	2	3	2D, 4D	80	-1.5	4.5	2	40	
9	WAKE03a	3 device, 1 row, 1.5D spacing (A)	3	3	1.5	n/a	10	2	10	1	2	2D, 4D	120	-1.5	3	3	40	
10	WAKE03b	3 device, 1 row, 2D spacing (B)	3	3	2	n/a	10	2	10	3	2	2D, 4D	120	-1.5	3.5	3	40	
11	WAKE03c	3 device, 1 row, 3D spacing (C)	3	3	3	n/a	10	2	10	3	2	2D, 4D	120	-1.5	4.5	3	40	
12	WAKE03d	3 device, 1 row, 1.5D spacing with waves (D)	3	3	1.5	n/a	10	2	10	3	2	2D, 4D	120	-1.5	3	3	40	
13	WAKE06a	6-10 device, 2 rows, 2D Y-spacing, 3D X-spacing (A)	6	10	2	3	10	5	13	2	2	2D, 4D	80	-1.5	3.5	2	40	
14	WAKE06b	6-10 device, 2 rows, 2D Y-spacing, 4D X-spacing (B)	6	10	2	4	10	6	14	2	2	2D, 4D	80	-1.5	3.5	2	40	
15	WAKE06c	6-10 device, 2 rows, 2D Y-spacing, 5D X-spacing (C)	6	10	2	5	10	7	15	2	2	2D, 4D	80	-1.5	3.5	2	40	
16	WAKE06d	6-10 device, 2 rows, 2D Y-spacing, 6D X-spacing (D)	6	10	2	6	10	8	16	2	2	2D, 4D	80	-1.5	3.5	2	40	
17	WAKE06e	6-10 device, 2 rows, 2D Y-spacing, 8D X-spacing (E)	6	10	2	8	10	10	18	2	2	2D, 4D	80	-1.5	3.5	2	40	
18	FLOW04a	Flow with weir and waves (A)	0							3	3	6, 7.5, 9	12	wall	wall	9	40	
19	FLOW04b	Flow with weir and waves (B)	0							3	3	6, 7.5, 9	12	wall	wall	9	40	
20	WAKE06f	6-10 device, 2 rows, 2D Y-spacing, 4D X-spacing, with waves (F)	6	10	2	4	10	6	14	3	2	2D	120	-1.5	3.5	3	40	
21	WAKE06g	6-10 device, 2 rows, 2D Y-spacing, 4D X-spacing, with waves (G)	6	10	2	4	10	6	14	3	2	2D	120	-1.5	3.5	3	40	
22	FLOW05	Baseflow with increased boundary layer turbulence	0							3	3	6, 7.5, 9	12	wall	wall	3	40	
23	WAKE06h	6-10 device, 2 rows, 2D Y-spacing, 4D X-spacing, BL turbulence (H)	6	10	2	4	10	6	14	3	2	2D	120	-1.5	3.5	3	40	
24	WAKE06i	6-10 device, 2 rows, 2D Y-spacing, 4D X-spacing, BL turbulence 2 (I)	6	10	2	4	10	6	14	3	2	2D	120	-1.5	3.5	3	40	
25	FLOW06	Baseflow in the wake of a conical island	0							3	3	6, 7.5, 9	12	wall	wall	3	40	
										3	3	6, 7.5, 9	12	wall	wall	9	40	
26	WAKE06j	6-10 device, 2 rows, 2D Y-spacing, 4D X-spacing, with island (J)	6	10	2	4	10	6	14	3	2	2D	120	-1.5	3.5	3	40	
27	WAKE06k	6-10 device, 2 rows, 2D Y-spacing, 4D X-spacing, with island 2 (K)	6	10	2	4	10	6	14	3	2	2D	120	-1.5	3.5	3	40	
28	WAKE09a	9-15 device, 3 rows, 2D Y-spacing, 4D X-spacing (A)	9	15	2	4	10	10	18	3	2	2D	120	-1.5	3.5	3	40	
29	WAKE09b	9-15 device, 3 rows, 2D Y-spacing, 5D X-spacing (B)	9	15	2	5	10	12	20	3	2	2D	120	-1.5	3.5	3	40	
30	WAKE09c	9-15 device, 3 rows, 2D Y-spacing, 6D X-spacing (C)	9	15	2	6	10	14	22	3	2	2D	120	-1.5	3.5	3	40	
31	WAKE09d	9-15 device, 3 rows, 2D Y-spacing, 4D X-spacing, with waves (D)	9	15	2	4	10	10	18	3	2	2D	120	-1.5	3.5	3	40	